

We thank the reviewers for their thoughtful reviews, which helped us to improve our manuscript. Point-by-point responses are provided as follows.

Reviewer 1:

Abstract: If most of the OC is secondary and Ca is predominantly primary, how can they have similar sources (line 32)? Is it that the precursor VOC has a similar source as Ca? Could it be that the species undergo similar atmospheric processing?

Response:

The reviewer's points are well taken. Accordingly, we have revised the sentence (line 29-31; note that the line number refers to the revised version of the manuscript) as follows. "Total OC was correlated with Ca (R^2 of 0.63), suggesting that OC precursors and Ca may have had similar sources, and the possibility that they underwent similar atmospheric processing."

Starting at Line 70: Is atmospheric re-suspended dust due to wind or human activity? If it is due to human activity is it "anthropogenic"?

Response:

It is likely that both mechanisms are important in controlling dust loadings. To remove the ambiguity, line 72 was revised as "In prior studies conducted in the Middle East, dust was identified as the major source of PM₁₀ (Givehchi, et al., 2013);"

The chosen cities for comparison in Table 1 seem randomly chosen, and this is probably not the case. Are these areas or their air quality similar to Riyadh in some way?

Response:

We sought observations of OC/EC measurements made in the last 10 years in urban areas world-wide. Urban areas may be hypothesized to have similar sources of PM, e.g. vehicular exhaust and industrial emissions, albeit that the nature of the PM will vary depending on factors such as local fleet and fuel mixes and local industry. Thus, the table title is revised as "Comparison of OC and EC concentrations ($\mu\text{g m}^{-3}$) measured in urban areas world-wide". In the revision, we added one more Korean urban city and replaced the US study with two large cities as follows below. We also compared our measurements with other studies in the Middle East expected to have similar climatological conditions as Riyadh.

Combining a response to this point and to Review 2, comment 3, the related main text (lines 237-254) was revised as follows:

"Table 1 presents some comparative values of measured EC and OC concentrations in PM_{2.5} in urban areas world-wide, since urban areas are expected to share some anthropogenic source types (e.g. vehicular and industrial emissions) with Riyadh. The average concentrations in this work for both EC and OC were remarkably consistent with those reported by von Schneidemesser et al. (2010) and Abdeen et al. (2014) for 11

Middle Eastern sampling sites, including Tel Aviv, a major city in Israel (OC: 4.8 and EC: 1.6 $\mu\text{g m}^{-3}$). The average OC concentrations in Riyadh were also comparable to those reported for suburban Hong Kong (4.7 $\mu\text{g m}^{-3}$, Huang et al., 2014b), higher than Cleveland and Detroit, US (3.10 and 3.54 $\mu\text{g m}^{-3}$, Snyder et al., 2010), but lower than those reported for Gwangju, Korea (5.0 $\mu\text{g m}^{-3}$, Batmunkh et al., 2016), Veneto, Italy (5.5 $\mu\text{g m}^{-3}$, Khan et al., 2016), Athens, Greece (6.8 $\mu\text{g m}^{-3}$, Grivas et al., 2012), urban Hong Kong (10.1 $\mu\text{g m}^{-3}$, Ho et al., 2006), Delhi, Indian (16.5 \pm 6.6 $\mu\text{g m}^{-3}$, Satsangi et al., 2012), and Beijing, China (18.2 \pm 13.8 $\mu\text{g m}^{-3}$, Zhao et al., 2013), reflective of the different mix of sources and different photochemical environments. EC concentrations also vary widely among urban regions, depending on the characteristics of local sources.”

City	Duration	EC		OC		References
		Conc. ($\mu\text{g m}^{-3}$)	S.D. ($\mu\text{g m}^{-3}$)	Conc. ($\mu\text{g m}^{-3}$)	S.D. ($\mu\text{g m}^{-3}$)	
Athens, Greece	Jan to Aug, 2003	2.2	6.8			Grivas et al., 2012
Gwangju, Korea	Winter of 2011	1.7	5.0	0.9	2.5	Batmunkh et al., 2016
Cleveland, US	Jul, 2007 and Jan, 2008	0.33	3.10	1	8	Snyder et al., 2010
Detroit, US		0.35	3.54	1	6	
Beijing, China	Selective days in four seasons from 2009 to 2010	6.3	18.2	2.9	13.8	Zhao et al., 2013
Urban, Hong Kong	Nov, 2000 to Feb, 2001 and Jun, 2001 to Aug, 2001	5.71	10.1	0.8	1.9	Ho et al., 2006
Suburban, Hong Kong	Mar, 2011 to Feb, 2012	0.86	4.7	0.5	2.8	Huang et al., 2014b
Veneto, Italy	Apr 2012 to Feb 2013	1.3	5.5			Khan et al., 2016
Delhi, India	Dec 20, 2012 to Feb 26, 2013	12.0	16.4	4.4	6.6	Panda et al., 2016
Middle East	Jan to Dec, 2007	2.1	5.3	2.2	4	von Schneidemesser, et al., 2010 Abdeen, et al., 2014
(11 sampling sites in Palestine, Jordan and Israel)						
Riyadh, Saudi Arabia	Apr to Sep, 2012	2.13	4.76	2.5	4.4	this study

References added:

Batmunkh, T., Lee, K., Kim, Y. J., Bae, M.-S., Maskey, S., Park, K.: Optical and thermal characteristics of carbonaceous aerosols measured at an urban site in Gwangju, Korea, in the winter of 2011, *J. Air & Waste Manage Association*, 66, 151-163, DOI: 10.1080/10962247.2015.1101031, 2016.

Snyder, D. C., Rutter, A. P., Worley, C., Olson, M., Plourde, A., Bader, R. C., Dallmann, T., Schauer, J. J.: Spatial variability of carbonaceous aerosols and associated source tracers in two cities in the Midwestern United States, *Atmos. Environ.*, 44, 1597-1608, 2010.

von Schneidmesser, E., Zhou, J., Stone, E. A., Schauer, J. J., Qasrawi, R., Abdeen, Z., Shpund, J., Vanger, A., Sharf, G., Moise, T., Brenner, S., Nassar, K., Saleh, R., Al-Mahasneh, Q. M., Sarnat, J.A.: Seasonal and spatial trends in the sources of fine particle organic carbon in Israel, Jordan, and Palestine, *Atmos. Environ.*, 44, 3669-3678, 2010.

Starting at line 276 “Since OC concentrations had no significant weekday-weekend variation, the increase in OC/EC ratio during the weekend likely indicates the importance of regional photochemical sources of SOC, although decreased NO_x emissions on weekends may promote more efficient photochemical processing of local SOC precursors” This is a curious conclusion to draw from Figures 5 and S2, but maybe not in the context of results discussed later in the manuscript. From these figures, it appears that changes in [EC] are what drive the changes in the OC/EC ratio predominantly. Perhaps the authors are intending to state primary OC emissions follow trends in EC and that the OC on Wednesdays is more primary than say on the weekends when SOC makes a larger contribution? It seems the authors allude to this when discussing figure 6. This needs to be shown first and the authors need to state the findings to support this statement more articulately.

Response:

Thank you for these helpful comments. We switched the order of sections 3.2 and 3.3 and “Diurnal variation of OC and EC” now comes before “Weekend effect in OC and EC concentrations”, as suggested.

Also, regarding this sentence:

“Since OC concentrations had no significant weekday-weekend variation, the increase in OC/EC ratio during the weekend likely indicates the importance of regional photochemical sources of SOC, although decreased NO_x emissions on weekends may promote more efficient photochemical processing of local SOC precursors (Gentner et al., 2012).” we have modified it as follows:

“OC concentrations had no significant weekday-weekend variation. The decrease of EC was the main driver of the increasing OC/EC ratio during the weekends, indicating reduced primary emissions and effective SOC formation / transport during the weekends.”

Why not explore the diurnal profiles also separated by weekend/weekday. That would help support the statements the authors make (above) regarding OC/EC findings.

Response:

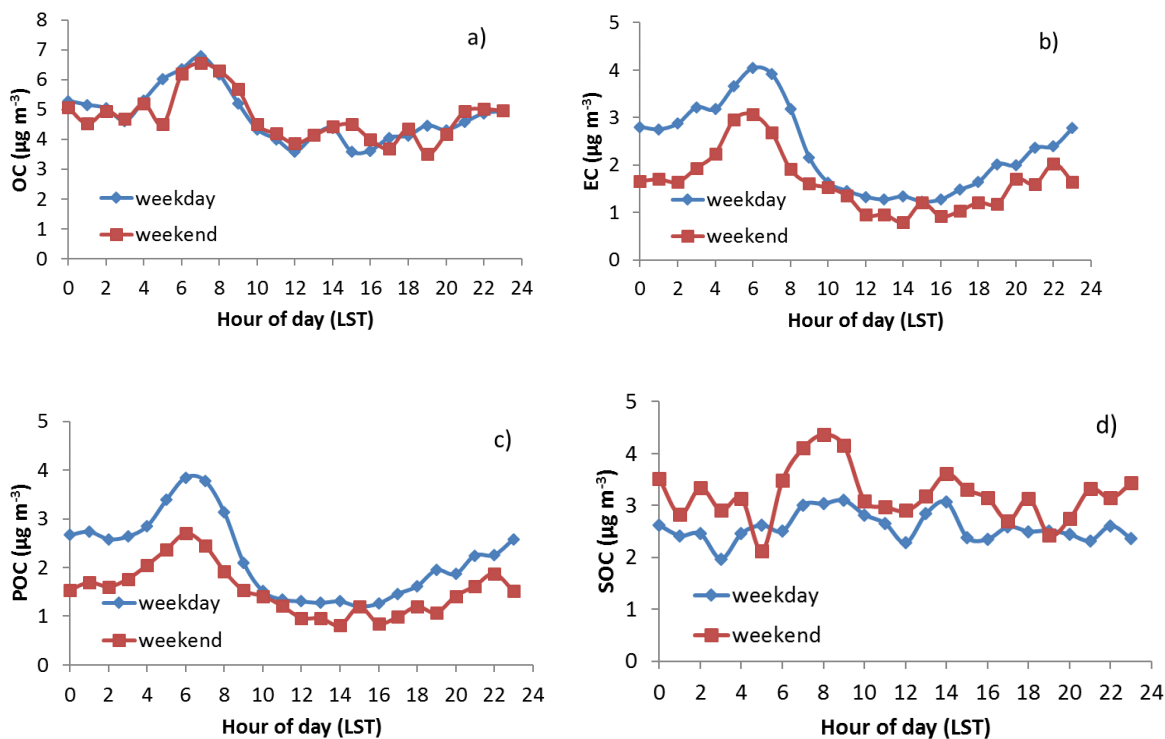
We replaced the original Fig. S3 with the following figure and added the corresponding discussion in lines 276 to 277:

“The diurnal variations of OC and EC on weekdays and weekends exhibited similar trends (Fig. S3), but EC was higher during weekdays.”

Lines 345 to 350:

“The diurnal variations of POC and SOC were similar on weekdays and weekends, but the weekday-to-weekend changes in POC and SOC had opposite trends. The estimated POC was $2.2 \pm 2.5 \mu\text{g m}^{-3}$ on weekdays and decreased to $1.5 \pm 1.9 \mu\text{g m}^{-3}$ on weekends. The estimated SOC was $2.6 \pm 2.9 \mu\text{g m}^{-3}$ on weekdays and increased by 23% to 3.2 ± 4.5

$\mu\text{g m}^{-3}$ on weekends. The elevated SOC during weekends was likely due to regional production and transport.”



Is it possible that if calcium carbonate forms, other compounds, for example would potassium carbonate form? It does seem from Figure 8 that there are two regimes for K vs. Ca. Does that inform the OC and Ca correlation analysis further?

Response:

Yes, it is possible that other carbonates were present. We revised lines 377 to 380 as follows:

“The correlation between Ca and other dust metal species (Al, Fe, K, Fe and Mg), however, showed two divergent regimes, suggestive of an additional Ca-containing source besides dust, that may have shared the same sources as OC.”

Editorial: Sometimes the authors use present tense (e.g., line 80) and sometimes past tense (e.g., line 216, 218) and it is distracting.

Response:

Revised accordingly.

We thank the reviewers for their thoughtful reviews, which helped us to improve our manuscript. Point-by-point responses are provided as follows.

Reviewer 2:

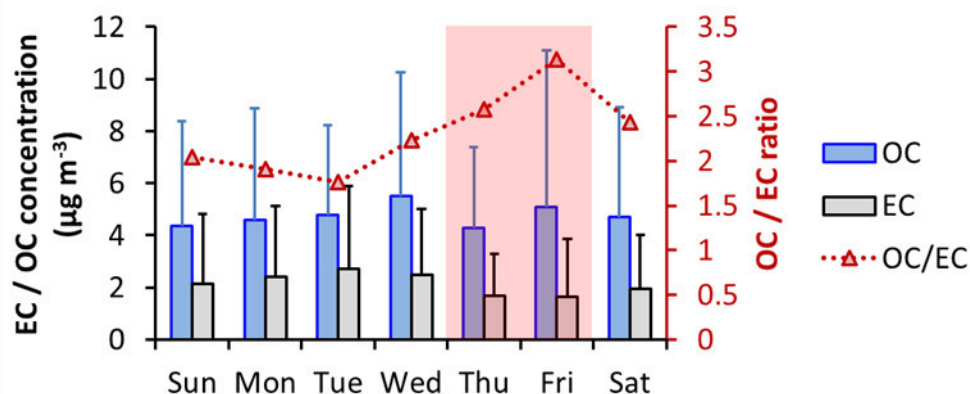
This is mostly an excellent submission, presenting results from a long-term measurement campaign in Saudi Arabia and source apportionment analysis. Questions I had were subsequently answered in the submission, which is usually a sign the authors have done a thorough job with the analysis. However, one glaring flaw appears to be that in 2012, the weekend in Saudi Arabia was Thu-Fri, not Fri-Sat. The authors should re-analyze their data accordingly. 2013 news article about the weekend switch: <http://english.ahram.org.eg/NewsContent/2/8/74730/World/Region/Saudi-Arabia-changes-working-week-to-SunThurs-Offi.aspx>

Response:

Thank you to the reviewer for pointing out this flaw.

Upon re-analyzing the data for the correct weekend dates, we discovered that the analysis was correct (i.e., the weekend was defined as Thu-Fri) but the labels in the figure were incorrect. The axis label in Fig. 5 (now Fig. 6) was updated as shown below. The main text (lines 289-293) has also been corrected:

“To investigate whether a weekend effect could be discerned in the Riyadh dataset, two-sample t-tests assuming unequal variances were performed for hourly EC and OC samples, grouped according to whether they were obtained on weekdays (Saturday to Wednesday) or on weekends (Thursday and Friday).”



1. How often or when was the OC/EC filter changed? Was the OC/EC correction different at the beginning than at the end? Did the switch coincide with particular days of the week?

Response:

OC/EC filters were changed after the laser intensity was reduced to 2000 or 3000 [a.u.] We have added a footnote to Table S1 to indicate this. The time to reach this threshold was mainly controlled by particulate concentrations, especially during dust storms. Some

filters lasted for only 24-48 hours, while some lasted for about 6-7 days. The OC/EC correction was the same over the entire filter lifetime, as long as there were refractive particles on the filters.

2. Lines 450-451 - the authors say the limited sample size means they can't quantify the local and regional contributions to OC and EC. However, this limitation only applies to the 24-hour metals analysis, which also appears to show that SOC, associated with Ca, may be regional. So couldn't the authors use the hourly-resolved OC/EC data to estimate local contributions to OC and EC?

Response:

We removed this sentence.

3. Table 1 could be rearranged to list the current study next to the 2007 middle-east study, as that is most relevant to the present analysis. I would have liked to see a more extensive comparison of the two sets of results.

Response:

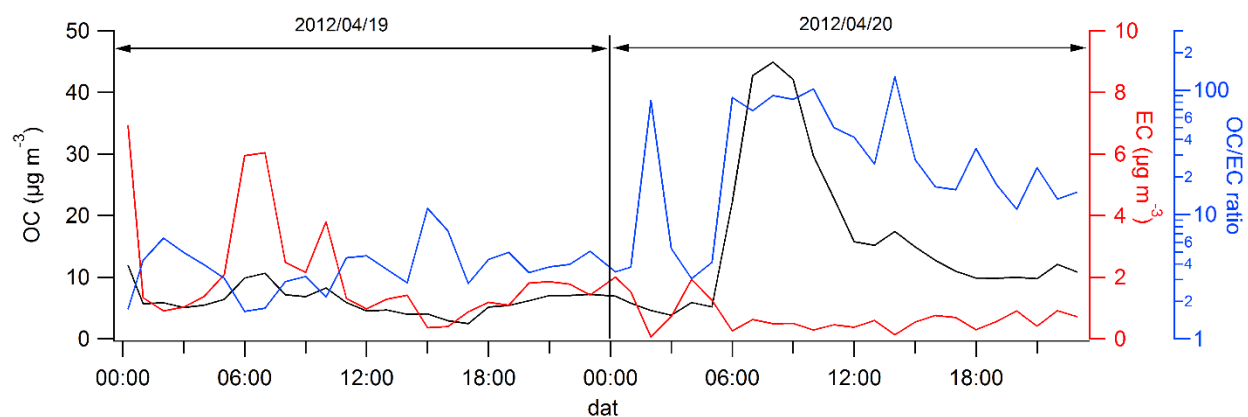
We have rearranged the table as suggested, revised the discussion of Table 1, lines 275-289.

4. Figures 2 and 3 just have EC/OC concentrations as the axis title, but the OC/EC ratios are also shown. Maybe put the ratio on the secondary axis with an appropriate title? Also, OC/EC ratios in the 100s - admittedly outliers - are interesting. Are those associated with low pollution levels?

Response:

Figs. 2 and 3 have been modified as suggested.

Most of the high OC/EC ratios (>100) were caused by rapid, large increases in OC and an accompanying decrease in EC during the measurement. An example is shown below, covering two consecutive days of data. On 2012/04/19, OC was $6.24 \pm 2.27 \mu\text{g m}^{-3}$, EC was $2.08 \pm 1.79 \mu\text{g m}^{-3}$, and OC/EC ratio was 4.11 ± 2.07 ; on 2012/04/20, OC increased to $16.09 \pm 12.20 \mu\text{g m}^{-3}$, EC decreased to $0.71 \pm 0.51 \mu\text{g m}^{-3}$, and the OC/EC ratio increased to 39.80 ± 37.37 . The highest OC/EC ratio on 2012/04/20 was 102. The total carbon on the second day was almost double that of the first day. This event may be a dust plume, as the methodology applied in the study cannot correct for carbonate interference in the OC/EC observations, although we have made inferences as to the presence of carbonate, as described in the text. While we do not have additional data to fully explore the causes of these excursions, we have no firm reason to remove these data, and thus we kept them in our dataset.



5. Figure 6(c) - Axis title is wrong. Also, the average ratios appear to be wrong, as almost all of them are higher than 75th percentile of the data. What do the caps represent - 90th or 95th or 99th percentile?

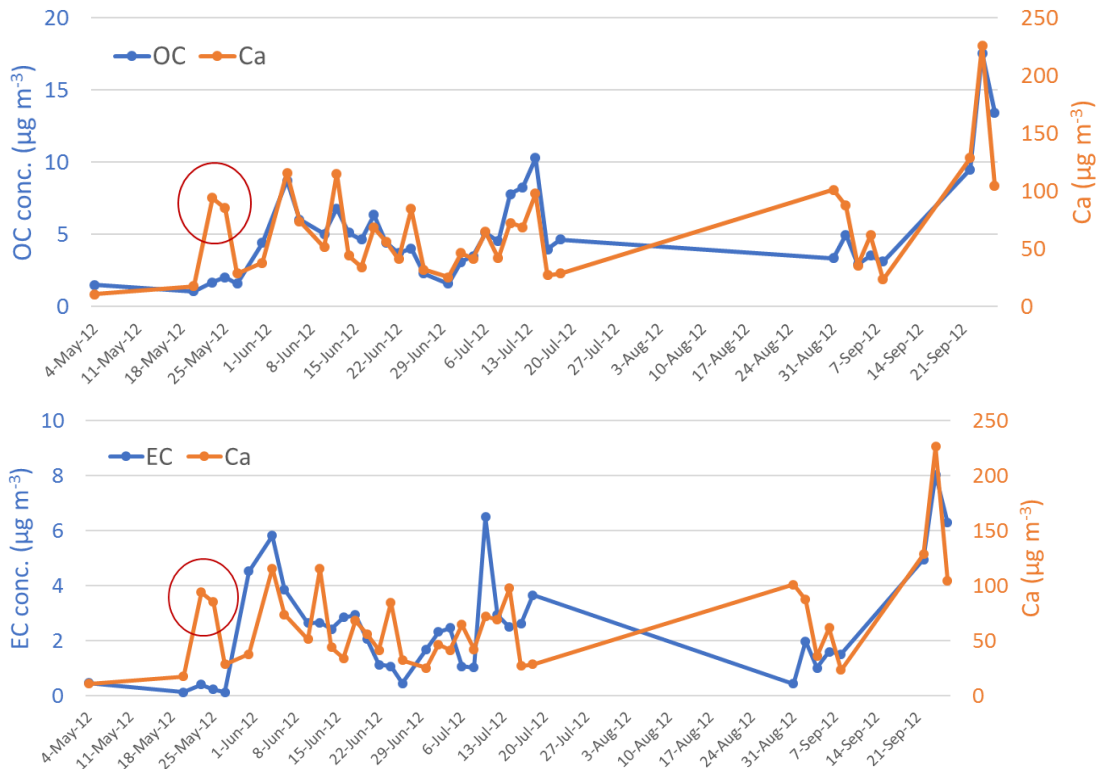
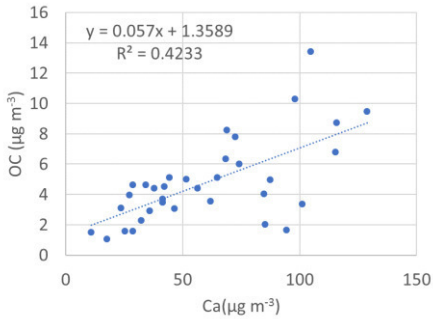
Response:

Thank you for pointing this out; we have corrected the y-axis title. The upper and lower caps represent 90th and 10th percentiles, respectively. The high average OC/EC ratios were caused by several individual high OC/EC ratios, as explained in comment 4. We retained the median and removed the point indicating the average in Fig. 5 (now Fig 6) to avoid confusion, and made similar changes to the other box-and-whisker figures.

6. Figure 8 - the high correlation between OC and Ca appears driven by a single high-value sample. Is that really good enough to push the OC-Ca connection?

Response:

Removing the high-value data point indeed decreased R^2 , however, the time series of OC and Ca matched each other well and better than that of EC and Ca (see the figures below). The relationship between OC and Ca looks to be real, but what caused the relationship was uncertain as we discussed in the main text: whether a methodology artifact or that these species actually shared the same source origins. We have included these time series in the supporting material to illustrate this relationship and modified the sentence 368-370 as follows “However, OC had a relatively strong correlation with Ca (R^2 of 0.63) (Fig. 8 and Fig. S7) but, similar to EC, a poor correlation with other dust species (not shown).”



7. Figure 11 - what happened to the samples in August? Also, maybe the Aug 31 sample should be grouped with September?

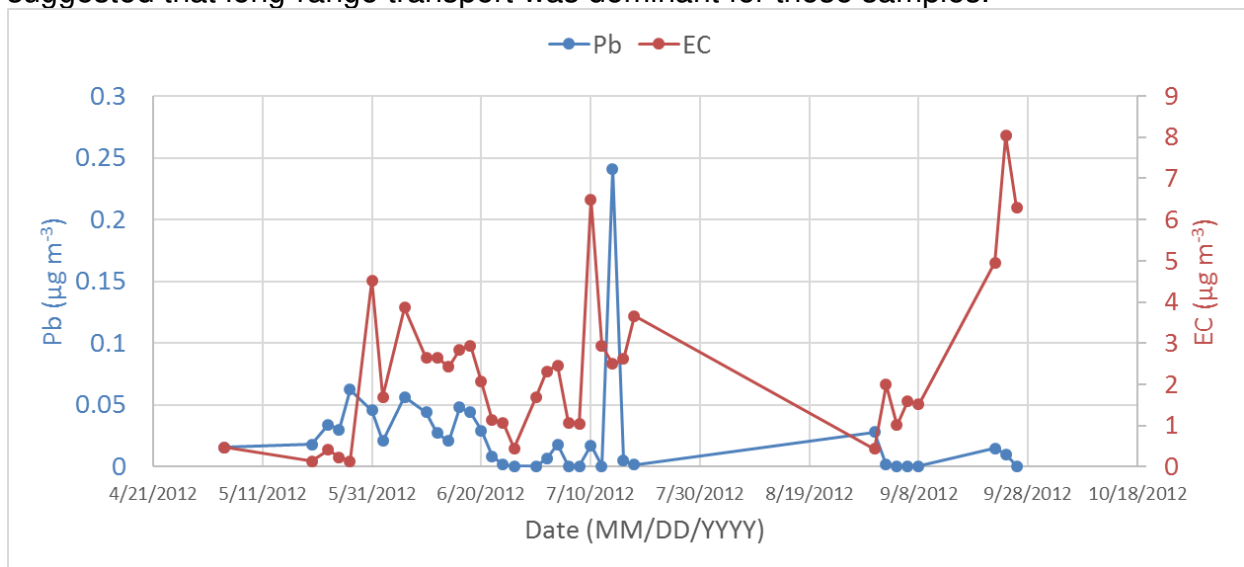
Response:

In 2012, Ramadan and Eid ran from July 20-August 24 and no measurements were made during this period. Thank you for the suggestion to regroup the Aug 31 sample with the September samples. We have done this and updated the numbers in lines 474 to 478. "The contribution of the mixed source ranged from 37% in May ($0.7 \mu\text{g m}^{-3}$) to 95% in September ($6.7 \mu\text{g m}^{-3}$). The EC concentration was also mainly attributed to the mixed source ($1.9 \mu\text{g m}^{-3}$, 92%)."

8. Figure 11 - was there no cement or gas flare or local vehicular contributions in May? That seems inconceivable. The authors should explain a bit more.

Response:

EC was indicated as a tracer for the mixed sources and Pb was the tracer for long-range transport, according to the PMF-resolved source profile (Figure 10). Daily-average EC concentrations were relatively low while Pb concentrations were high in May samples compared with those in the other periods, as shown in the following figure. This suggests that long range transport was dominant at that time. Due to the limited number of samples, PMF was unable to pick up the low contribution from mixed sources, with the result that minimal cement / gas flare / local vehicular contributions were found for most May samples. Lines 478 to 480 are revised as follows, “In some May samples, the mixed source contribution was negligible, as the source tracer, EC, was only 0.1-0.4 $\mu\text{g m}^{-3}$, about one order of magnitude lower than that in other periods. The tracer analysis suggested that long-range transport was dominant for those samples.”



9. Figure A.2 shows that all the corrected laser values increase in transmittance at the beginning, which is rather strange - no EC should have left the filter in He1! What is going on - is the correction wrong?

Response:

Figure A.2a shows a thermogram for one of the “aged” blank samples. As expected, negligible carbon was detected in this sample, but the refractive particles that remained on the filter from previous samples still significantly influenced the laser variation. Fig. A.1a shows that the quadratic fit could not reproduce the signal at low temperature (<200 °C), so the increasing corrected laser signal during the He1 and He2 phases is likely an artifact of the correction methodology, and may not indicate EC evolution. However, we note that the studies of Wang et al. (2010) and Bladt et al. (2012) showed that refractory metal oxides / salts may cause premature EC evolution in an inert environment, thereby increasing the laser signal. A high loading of dust metals on the filters in our Riyadh samples may thus have caused premature EC evolution during the He stage. If this were the case, the original variable laser signal that we showed was

dependent on temperature may have masked that phenomenon, while the corrected one revealed it.

We revised the main text from lines 561 to 570 as follows:

“It is noted that although the quadratic equation correction produced a better laser signal for purposes of the carbon analyses, this correction did not work perfectly in the low temperature He phase, where the corrected laser signals exhibited unexpected increases. However, this shortcoming did not substantially influence the accuracy of the correction during subsequent carbon evolution. We note that premature evolution of EC, leading to an increasing laser signal in the inert environment due to the existence of refractory metal oxides, was observed in the studies of Wang et al. (2010) and Bladt et al. (2012). The increases in the corrected laser signal during the He stage in this study may be partially due to the same cause, as Riyadh samples contained abundant metal oxides.”

Reference:

Bladt, H., Schmid, J., Kireeva, E.D., Popovicheva, O. B., Perseantseva, N. M., Timofeev, M. A., Heister, K., Uihlein, J., Ivleva, N. P., Niessner, R: Impact of Fe Content in Laboratory-Produced Soot Aerosol on its Composition, Structure, and Thermo-Chemical Properties, *Aerosol Sci. Tech.*, 46, 1337-1348, DOI:10.1080/02786826.2012.711917, 2012.

Wang, Y., Chung A., Paulson, S.E.: The effect of metal salts on quantification of elemental and organic carbon in diesel exhaust particles using thermal-optical evolved gas analysis, *Atmos. Chem. and Phys.*, 10, 11447-11457, 2010.

Sources of PM_{2.5} carbonaceous aerosol in Riyadh, Saudi Arabia

Qijing Bian¹, Badr Alharbi², Mohammed M. Shareef³, Tahir Husain³, Mohammad J. Pasha¹, Samuel A. Atwood¹, Sonia M. Kreidenweis^{1,*}

¹Department of Atmospheric Science, Colorado State University, Fort Collins, CO, 80526, USA.

²National Center for Environmental Technology, King Abdulaziz City for Science and Technology, P.O. Box 6086, Riyadh 11442, Saudi Arabia.

³Faculty of Engineering and Applied Science, Memorial University, St. John's, NL, A1B 3X5 Canada.

*Corresponding author: bianqj@atmos.colostate.edu and sonia@atmos.colostate.edu

Abstract

Knowledge of the sources of carbonaceous aerosol affecting air quality in Riyadh, Saudi Arabia is ~~was~~ limited, but needed for the development of pollution control strategies. We conducted sampling of PM_{2.5} from April to September, 2012 at various sites in the city, and used a thermo-optical semi-continuous method to quantify the organic carbon (OC) and elemental carbon (EC) concentrations. The average OC and EC concentrations were 4.7 ± 4.4 and 2.1 ± 2.5 $\mu\text{g m}^{-3}$, respectively, during this period. Both OC and EC concentrations had strong diurnal variations, with peaks at 6-8 am and 20-22 pm, attributed to the combined effect of increased vehicle emissions during rush hour and the shallow boundary layer in the early morning and at night. This finding ~~suggests-suggested~~ a significant influence of local vehicular emissions on OC and EC. The OC/EC ratio in primary emissions was estimated to be 1.01, close to documented values for diesel emissions. Estimated primary (POC) and secondary (SOC) organic carbon concentrations were comparable, with average concentrations of 2.0 ± 2.4 and 2.8 ± 3.4 $\mu\text{g m}^{-3}$, respectively.

We also collected 24 hour samples of PM₁₀ onto quartz microfiber filters and analyzed these for an array of metals by ICP-OES. Total OC was correlated with Ca (R^2 of 0.63), suggesting ~~that they OC precursors and Ca~~ may have similar sources, ~~and the possibility that they underwent the similar atmospheric progressprocessing~~. In addition to a ubiquitous dust source, Ca is emitted during desalting processes in the numerous refineries in the region and from cement kilns, suggesting these sources may also

34 contribute to observed OC concentrations in Riyadh. Concentration weighted trajectory
36 (CWT) analysis showed that high OC and EC concentrations were associated with air
masses arriving from the Persian Gulf and the region around Baghdad, locations with
38 high densities of oil fields and refineries as well as a large Saudi Arabian cement plant.
We further applied positive matrix factorization to the aligned data set of EC, OC and
40 metal concentrations (Al, Ca, Cu, Fe, K, Mg, Mn, Na, Ni, Pb and V). Three factors were
derived, and were proposed to be associated with oil combustion, industrial emissions
42 (Pb-based), and a combined source from oil fields, cement production, and local vehicular
emissions. The dominant OC and EC source was the combined source, contributing 3.9
 $\mu\text{g m}^{-3}$ (80%) to observed OC and 1.9 $\mu\text{g m}^{-3}$ (92%) to observed EC.

44 **1. Introduction**

Organic carbon (OC) and elemental carbon (EC) (or black carbon, BC, operationally
46 identified based on detection method) are key components of the atmospheric aerosol
(Jacobson et al., 2000). The contribution of carbonaceous components to total particulate
48 matter (PM) concentrations varies with site and season, comprising from 20 to 90% of the
total mass (Kanakidou, et al., 2005). EC is emitted from a variety of combustion processes
50 (Bond et al., 2013), is classified as a short-lived climate forcer that contributes to
atmospheric warming (Ramanathan and Carmichael, 2008), and is also associated with
52 human morbidity and mortality (Weinhold, 2012). OC includes both direct emissions
(primary organic carbon, POC) and secondary OC (SOC) formed in the atmosphere via
54 oxidation (Robinson et al., 2007). Common sources of atmospheric POC and of SOC
precursors are vehicular exhaust, industrial emissions, biogenic emissions, and biomass
56 burning (Millet et al., 2005; Saarikoski et al., 2008; Genberg et al., 2011; Hu et al., 2012;
Vodička et al., 2013; Heal and Hammonds, 2014; Huang et al., 2014a, b). Except near
58 strong emission sources, secondary organic aerosol is the main contributor to the total
organic aerosol mass concentration, frequently accounting for 72±21% (Zhang et al. 2007;
60 Jimenez et al., 2009).

Trace metals account for only a small fraction of PM mass concentrations, but they can
62 adversely impact human health (e.g., Lippmann et al., 2006; Hong et al., 2010). As some
emission sources release specific trace elements, these elements can serve as useful
64 source markers in PM source apportionment studies (Lee et al., 2011; Peltier and
Lippmann, 2010; Han et al., 2005; Harrison et al., 2012; Karanasiou et al., 2009; Ondov
66 et al., 2006; Querol et al., 2007; Viana et al., 2008; Yu et al., 2013). Elemental
enrichments can also be used to roughly differentiate natural and anthropogenic sources
68 (Khodeir et al., 2012; Rushdi, et al., 2013). Relative abundances of crustal elements can
help identify the sources of suspended dust, as these abundances are known to be
70 different for different dust source regions (Engelbrecht et al., 2009).

In this study, we report measurements of ambient particulate matter in Riyadh, the capital of Saudi Arabia. In prior studies conducted in the Middle East, dust ~~re-suspended dust~~ is was identified as the major source of PM₁₀ (~~Ginoux, et al., 2012~~; Givehchi, et al., 2013); however, contributions from anthropogenic sources to PM mass concentrations ~~are were~~ found to be significant ~~(~~>82% of total PM₁₀ mass, Al-Dabbous and Kumar, 2015; >50% of PM₁₀ Tsiouri et al., 2015). Tsiouri et al. (2015) summarized the major sources of PM₁₀ in ambient air in the Middle East as oil combustion, re-suspended soil, road traffic, crustal dust, and marine aerosol; significant sources of PM_{2.5} were oil combustion in power plants, re-suspended soil, sand dust, and road traffic. Carbonaceous particles were estimated to account for 50-60% of PM_{2.5} in cities in Palestine, Jordan, and Israel (Abdeen et al., 2014). Not surprisingly, since oil production and processing ~~is was~~ widespread across the Middle East, heavy oil combustion was estimated to contribute 69% to PM_{2.5} mass and 18% to PM₁₀ in Jeddah, Saudi Arabia (Khodeir et al., 2012). Air quality in Riyadh reflects not only the impact of local and regional dust and regional oil extraction and refining, but also significant local sources that include a heavy traffic load and multiple industries. We focus here on identifying the major sources of PM_{2.5} carbonaceous aerosol in Riyadh to provide a basis for formulating air pollutant mitigation strategies.

2. Methodology

2.1 Sampling sites and data collection

Riyadh and its environs were divided into 16 12 km × 12 km sampling cells as shown in Fig. 1. Sampling locations within each cell were carefully chosen to best represent the mix of land use and other characteristics of the cell. From April through September, 2012, an in-situ semi-continuous OC/EC analyzer (Sunset Laboratory Inc., Model-4), installed in a mobile laboratory, moved from cell to cell and measured hourly EC and OC, with some interruptions due to instrument maintenance or holidays. The sampling strategy is documented in Table S1. In this instrument, volatile gases ~~are were~~ removed from the samples by carbon denuders prior to collection. Airborne particles smaller than 2.5 μm ~~we~~ are then collected on quartz fiber filters at a flow rate of 8 l min⁻¹. Upon completion of a preset sampling duration, all carbon that ~~had~~ been accumulated on the filter ~~is was~~ removed by heating the sample in multiple increasing temperature steps, first in a completely oxygen-free helium environment and then in a He/O₂ environment. The vaporized compounds flow ~~ed~~ through an oxidizer oven, ~~are were~~ oxidized to carbon dioxide, and ~~we~~ are detected via an infrared analyzer. An external methane (CH₄) standard ~~is was~~ injected at the end of every analysis and used to normalize the analytical result. Since in theory the quartz filter has had all of the collected carbonaceous aerosol removed during each analysis cycle, the filter ~~is was~~ re-used for multiple samples and changed only periodically.

110 A detailed description of the PM₁₀ sample collection and elemental analysis
112 methodologies can be found in Alharbi et al. (2015). In brief, sampling was conducted
114 from the same mobile platform and concurrent with the OC/EC sampling. A PM₁₀ inlet
116 was used to sample ambient aerosol onto quartz microfiber filters over a 24 h period.
These samples were collected every three days and elemental analyses for Al, As, B, Ca,
Cd, Co, Cr, Cu, Fe, K, Li, Mg, Mn, Mo, Na, Ni, Pb, Te, V, and Zn were performed by ICP-
OES. NO and NO₂ (NO_x) were measured by chemiluminescence and O₃ was measured
by UV photometer simultaneously using Signal Ambirak air quality monitoring system
(Signal Ambitech Ltd, UK).

118 2.2 EC and OC re-split method

The Sunset semi-continuous EC/OC analyzer adopts the same thermal-optical analysis
120 method for determination of OC and EC that is commonly applied to the offline analysis
122 of filter samples. The OC and EC mass concentrations (as mass of C) are quantified by
124 a calibrated non-dispersive infrared sensor (NDIR) signal that detects the evolved CO₂.
Ideally, OC is defined as the carbon evolved under increasing temperature ramps
126 conducted in an inert atmosphere (100% He) and EC is defined to be the subsequent
128 carbon evolution in an oxidizing atmosphere (He/10% O₂ mixture). In the inert
atmosphere, rather than simply volatilizing, a fraction of OC may be pyrolyzed due to
insufficient oxygen, and this pyrolyzed OC may be evolved in the subsequent oxidizing
atmosphere, appearing as EC. This fraction of OC is usually called pyrolyzed organic
carbon (PyOC). To subtract PyOC from EC, laser transmittance or reflectance is deployed
130 to monitor the variations in filter darkness; the transmittance or reflectance responds to
the presence of EC throughout the analysis, but then drops when PyOC is formed and
132 rises again as PyOC is evolved. The fraction of total assigned EC evolved in the oxidizing
atmosphere before the laser signal returns to its initial value is believed to be due to PyOC,
134 so in post-analysis the final EC is reported as the difference between the total carbon
evolved in the oxidizing atmosphere and the PyOC. This methodology has been
136 automated in the Sunset instrument. However, unusual EC and OC splits for a large
number of samples were observed during the study period: (a) split points jumped to the
138 end of the analysis because the laser response did not rebound to its initial value before
the CH₄ calibration phase; or (b) split-points were located in the pre-oxygen position.
140 These split point deviations [may be ascribed](#) to refractory residue on the filters: the
laser correction factor supplied in the standard manufacturer software may not be
142 applicable to the dusty environment of Riyadh (Polidori et al., 2006; Jung et al., 2011;
Wang et al., 2012). Therefore, observed relationships between laser response and
144 temperature in the CH₄ + O₂ injection calibration phase were used to develop a corrected
split point. The correction methodology assumed that only refractory material was present
146 on the filter in this phase, so that effects of this refractory material on the laser response
to temperature variations could be isolated, corrected, and these corrections applied

148 during the other analysis phases. A full description of the methodology is found in the
Appendix. We noted, however, that measurement artifacts from carbonates in dust may
150 ~~be~~ have been present in this study, which would result in a high bias in the OC
measurements. As noted in Karanasiou et al. (2011) and in the standard operating
152 procedure (SOP) document published by the Research Triangle Institute (RTI)
([https://www3.epa.gov/ttnamti1/files/ambient/pm25/spec/RTIIMPROVEACarbonAnalysis](https://www3.epa.gov/ttnamti1/files/ambient/pm25/spec/RTIIMPROVEACarbonAnalysisSSLSOP.pdf)
154 [SSLSOP.pdf](https://www3.epa.gov/ttnamti1/files/ambient/pm25/spec/RTIIMPROVEACarbonAnalysisSSLSOP.pdf)), the evolution of carbonates from filter samples during thermal analysis can
occur over several carbon peaks. While it is preferred to use acid decomposition of
156 carbonates (on separate sample punches) to obtain the best quantification, Karanasiou
et al. (2011) demonstrated that the protocol used in this study completely evolves
158 carbonates in the OC fraction, and that manual integration to isolate the carbonate
concentration ~~is~~ was possible but carries large uncertainty. Hence, we ~~do~~ did not attempt
160 to separately quantify carbonate in this work.

2.3 SOC estimation by minimum R squared (MRS) method

162 The EC tracer method is widely used to estimate secondary organic carbon mass
concentrations, applying the following equations, which assume that EC has only
164 combustion sources:

$$POC = \left(\frac{OC}{EC}\right)_{pri} \times EC \quad \text{Eqn 1}$$

$$166 \quad SOC = OC_{total} - \left(\frac{OC}{EC}\right)_{pri} \times EC - b \quad \text{Eqn 2}$$

where $(OC/EC)_{pri}$ is the OC/EC ratio in fresh combustion emissions, b denotes non-
168 combustion-derived POC, and OC_{total} and EC are ambient measurements. The key to
successful application of this method is to begin with an appropriate estimate of the
170 $(OC/EC)_{pri}$ ratio. Several approaches have been documented to determine $(OC/EC)_{pri}$.
Gray et al. (1986) directly adopted the ratios from emission inventories. Turpin and
172 Huntzicker (1995) used the measured OC/EC ratio when local emissions were dominant
in a certain location or over a specified period. Based on the expectation that co-emitted
174 POC and EC are well correlated, Lim and Turpin (2002) took the slope of OC against EC
using OC/EC ratio data for the lowest 5-10% values of that ratio. Millet et al. (2005)
176 proposed that a critical point where SOC ~~is~~ was independent of EC should represent the
primary OC/EC ratio; the critical point ~~is~~ was found by a minimum R-squared (MRS)
178 method. Assuming that non-combustion sources (i.e., the b term in Eqn 2) are negligible,
this method can derive the most accurate primary OC/EC ratio, compared with previously-
180 proposed approaches (Wu and Yu, 2016). However, this method may underestimate the
SOC concentration if some SOC is associated with EC: co-emitted semi-volatile POC
182 could rapidly oxidize to low-volatility SOC and partition on the surface of EC. However,
given that accurate emission inventories ~~are~~ were not available for Riyadh, we employed

184 this method in the absence of a priori knowledge of $(OC/EC)_{pri}$ to provide a conservative
estimate of the SOC concentration during our observational period.

186 The methodology for and applications of the MRS method were documented in Millet et
al., (2005), Hu et al., (2012), and Wu and Yu (2016). The non-combustion source (*b* term)
188 ~~is was~~ assumed to be zero. A series of coefficients of determination (R^2) between EC and
SOC calculated by Eqns 1 and 2, varying $(OC/EC)_{pri}$ from 0 to 10 using steps of 0.01 in
190 the ratio, ~~is was~~ generated. At low $(OC/EC)_{pri}$ ratio, a significant portion of the estimated
SOC still belonged to POC. At high $(OC/EC)_{pri}$ ratio, the term $(OC/EC)_{pri} \times EC$ largely
192 ~~exceeds exceeded~~ OC_{total} and became dominant. At the correct ratio, all the POC
~~has been was~~ removed and R^2 of SOC and EC reached a minimum. This ratio ~~is was~~
194 then used to estimate SOC in all samples.

2.4 Back trajectory analysis

196 To develop an understanding of potential regional influences on observed PM, we
calculated 24-hr back trajectories (BTs) every 3 hours during each sampling period using
198 the National Oceanic and Atmospheric Administration (NOAA) Hybrid Single-Particle
Lagrangian Integrated Trajectory (HYSPLIT; Stein, et al., 2015; Rolph, 2016). Trajectories
200 were initiated for a starting height of 500 m above ground level (AGL). Residence time
analysis (RTA), describing the probability of air mass origins, was also performed
202 (Ashbaugh et al., 1985). The probability (P_{ij}), representing the residence time of a
randomly selected air mass in the ij^{th} cell during the observational period, ~~can be was~~
204 calculated as follows:-

$$P_{ij} \cong \frac{n_{ij}}{N} \quad \text{Eqn 3}$$

206 where n_{ij} is the number of trajectory segment endpoints that fell in the ij^{th} cell and N is the
total number of endpoints.

208 Concentration weighted trajectory analysis (CWT) is another effective tool ~~that we~~
combined with back trajectory data and pollutant concentration to trace the source origin
210 for certain species. The calculation formula is as follows:-

$$C_{ij} = \frac{1}{\sum_{i=1}^M \tau_{ijl}} \sum_{i=1}^M C_i \tau_{ijl} \quad \text{Eqn 4}$$

212 where C_{ij} is the average weighted concentration in the grid cell (i, j), C_i is the measured
species concentration, τ_{ijl} is the number of trajectory endpoints in the grid cell (i, j) and M
214 is the number of samples that have trajectory endpoints in the grid cell (i, j).

2.5 Positive matrix factorization (PMF) analysis

216 Positive matrix factorization (PMF) has been successfully applied to aerosol composition
218 data to suggest sources impacting the sampling site (Reff et al., 2007 and Viana et al.,
2008). We aligned daily-average OC and EC with concurrent averaged measurements of
220 metal concentrations in the PM₁₀ fraction (Al, Ca, Cu, Fe, K, Mg, Mn, Na, Ni, Pb and V)
and prepared a matrix ~~with of~~ size ~~of~~ 35 × 13 for input to the USEPA PMF, version 5.0
(https://www.epa.gov/air-research/positive-matrix-factorization-model-environmental-
222 data-analyses). Data points with “ND” were replaced by ½ of the detection limit and the
corresponding uncertainties were assigned as 5/6 of the detection limit. The uncertainties
224 for all other data were calculated as $s_{ij} + DL_{ij}/3$, where s_{ij} represents the analytical
uncertainty for species i in the sample j and DL_{ij} represents the detection limit (Polissar
226 et al., 1998; Reff et al., 2007). In this study, the analytical uncertainty was assumed to be
5% of the corresponding concentration for metal species. Uncertainties for the EC and
228 OC data were not reported. Norris et al. (2014) suggested that, for such cases, the initial
uncertainties be set to a proportion of the concentration. The uncertainties for OC and EC
230 were therefore calculated as 10% of the corresponding concentrations for this study.

3. Results and discussion

232 3.1 Overview of EC and OC concentrations

Fig. S1.a shows the time series of OC and EC concentrations during the study period and
234 denotes the corresponding sampling cells in which the measurements were obtained.
Average OC and EC concentrations during the observational period were 4.8 ± 4.4 and
236 $2.1 \pm 2.5 \mu\text{g C m}^{-3}$, respectively (we will use $\mu\text{g m}^{-3}$ for OC and EC hereafter when referring
to $\mu\text{g C m}^{-3}$). Table 1 presents some comparative values of measured EC and OC
238 concentrations in PM_{2.5} in urban areas world-wide, since urban areas are expected to
share some similar anthropogenic source types (e.g. vehicular and industrial emissions)
with Riyadh. The average concentrations in this work for both EC and OC were
240 remarkably consistent with those reported by von Schneidemesser et al. (2010) and
Abdeen et al. (2014) for 11 Middle Eastern sampling sites, including Tel Aviv, a major
city in Israel (OC: 4.8 and EC: 1.6 $\mu\text{g m}^{-3}$). The average OC concentrations were also
242 comparable to those reported for suburban Hong Kong ($4.7 \mu\text{g m}^{-3}$, Huang et al., 2014b),
higher than Cleveland and Detroit, US (3.10 and 3.54 $\mu\text{g m}^{-3}$, Snyder et al., 2010), but
244 lower than those reported for Gwangju, Korea (5.0 $\mu\text{g m}^{-3}$, Batmunkh et al., 2016), Veneto,
Italy ($5.5 \mu\text{g m}^{-3}$, Khan et al., 2016), Athens, Greece ($6.8 \mu\text{g m}^{-3}$, Grivas et al., 2012),
246 urban Hong Kong ($10.1 \mu\text{g m}^{-3}$, Ho et al., 2006), Delhi, Indian ($16.5 \pm 6.6 \mu\text{g m}^{-3}$, Satsangi
et al., 2012), and Beijing, China ($18.2 \pm 13.8 \mu\text{g m}^{-3}$, Zhao et al., 2013), reflective of the
250 different mix of sources and different photochemical environments. EC concentrations
were similar to those in Athens, Greece, higher than those reported for Veneto, Italy and
suburban Hong Kong, and lower than all other measurements shown in Table 1 EC
252 concentrations also vary widely among urban regions, depending on the characteristics
of local sources.

256 The Riyadh sampling site characteristics and the corresponding average OC and EC
257 concentrations in each grid cell are summarized in Table S1. Results of a one-sided t-test
258 ($p < 0.001$) on OC and EC data from industrial and residential sites suggested a significant
259 difference in carbonaceous aerosol concentrations between the two site types: OC mass
260 concentrations in industrial sites were 1.4 times those in the residential sites, and EC
261 mass concentrations were 1.7 times higher (Fig. 2). The mean OC/EC ratio was lower in
262 the industrial sites (3.1) than in residential sites (6.0), suggesting the importance of POC
263 emissions in industrial regions and a larger SOC contribution in residential areas. We also
264 divided Riyadh into four quadrants to investigate the spatial variation of OC and EC across
the city. Fig. 3 shows that OC and EC concentrations were higher in the eastern quadrants.

265 Fig. 4 shows the results of the RTA, demonstrating that air masses arriving in Riyadh
266 were mainly from within Saudi Arabia and from the south / southwest of the city in April
267 and May, and from the north / northeast from June to September, extending to the west
268 coast of the Persian Gulf. These two dominant wind directions ~~have been~~ were used to
stratify data in Fig. S1b, which shows that the average OC concentration increased from
270 3.8 to 5.3 $\mu\text{g m}^{-3}$ and EC from 1.1 to 2.7 $\mu\text{g m}^{-3}$ when the air mass source region shifted
from south/southeast to north/northeast, respectively.

272 3.3.2 Diurnal variation of OC and EC

273 Fig. S5 shows the diurnal variations in OC and EC mass concentrations. OC and EC
274 concentrations peaked from 6-9 am and were elevated during nighttime (after 1600 pm).
275 NO_x also showed a similar diurnal pattern (Fig. S2). The morning peak coincided with
276 traffic rush hours. ~~Fig. S3 showed that the diurnal variations of OC and EC on weekdays~~
277 and weekends exhibited the similar trends (Fig. S3), but EC was higher during weekdays.
278 The elevation of OC, EC and NO_x at night after 1600 pm may be attributed to the
279 accumulation of pollutants in the shallower nocturnal boundary layer. Average OC/EC
280 ratios showed no obvious trends; however, the median OC/EC ratio decreased slightly
281 over the time period when OC and EC concentrations built up, probably due to the
282 increased contributions from primary emissions. The average OC/EC ratio had a peak
283 around 14:00 pm, corresponding with peak concentrations of O₃, suggestive of secondary
284 aerosol formation.

Formatted: Highlight

Formatted: Highlight

Formatted: Highlight

Formatted: Highlight

286 3.2.3 Weekend effect in OC and EC concentrations

287 A “weekend effect” in concentrations of traffic-derived PM has been noted in previous
288 studies (e.g. Grivas et al., 2012; Bae et al., 2004; Moteballi et al., 2003; Lim and Turpin,
2002; Jeong et al., 2004; Lough et al., 2006). To investigate whether a weekend effect
290 ~~can~~ could be discerned in the Riyadh dataset, two-sample t-tests assuming unequal
variances were performed for hourly EC and OC samples, grouped according to whether

292 they were obtained on weekdays (~~Sunday-Saturday~~ to ~~Thursday~~Wednesday) or on
294 weekends (~~Thursday and Friday~~ and ~~Saturday~~). The test indicated a statistically
296 significant difference (29% lower on weekends) in EC concentrations between weekday
298 and weekend, but no significant difference in OC ($p < 0.001$ with a 95% confidence level),
300 as shown in Fig. 56. NO_x concentrations were also reduced during weekends, by 48%
302 compared to weekdays (Fig. S2S4). This reduction may be ascribed to the decrease in
304 vehicular activities and industrial activities during the weekend. ~~Since OC concentrations
had no significant weekday-weekend variation, the increase in OC/EC ratio during the
weekend likely indicates the importance of regional photochemical sources of SOC,
although decreased NO_x emissions on weekends may promote more efficient
photochemical processing of local SOC precursors (Gentner et al., 2012). OC
concentrations had no significant weekday-weekend variation. The decrease of EC was
the main driver of the increasing OC/EC ratio during the weekends, indicating the reduced
primary emission and effective SOC formation / transport during the weekends.~~

Formatted: Highlight

3.3 Diurnal variation of OC and EC

308 Fig. 6 shows the diurnal variations in OC and EC mass concentrations. OC and EC
310 concentrations peaked from 6-9 am and were elevated during nighttime (after 1600 pm).
312 NO_x also shows a similar diurnal pattern. The morning peak coincides with traffic rush
314 hours. The elevation of OC, EC and NO_x at night after 1600 pm may be attributed to the
316 accumulation of pollutants in the shallower nocturnal boundary layer. Average OC/EC
ratios showed no obvious trends; however, the median OC/EC ratio decreased slightly
over the time period when OC and EC concentrations built up, probably due to the
increased contributions from primary emissions. The average OC/EC ratio had a peak
around 14:00 pm, corresponding with peak concentrations of O_3 , suggestive of secondary
aerosol formation.

3.4 SOC estimation

318 Fig. 7 shows the determination of $(\text{OC}/\text{EC})_{\text{pri}}$ using the minimum R squared method
320 (MRS). The value of this ratio derived in this study ~~was~~ is 1.01, which occurred at the 14th
322 percentile in the observed OC/EC ratios. In the compilation of $\text{PM}_{2.5}$ OC and EC emission
324 profiles presented by Chow et al. (2011), the $(\text{OC}/\text{EC})_{\text{pri}}$ for oil combustion ~~was~~ is
documented to range from 0.2 to 2.5 with an average of 1.0 ± 0.2 , 0.9 to 8.1 with an
average of 3.4 ± 2.2 for gasoline emissions, and 0.2 to 2.7 with an average of 1.0 ± 0.8 for
326 diesel emissions. Our estimate ~~is was~~ is within with these ranges and ~~is was~~ is closer to the
328 averages for oil combustion and diesel emissions, consistent with expected important
contributions from these sources to $\text{PM}_{2.5}$ carbonaceous aerosol in Riyadh. Using our
MRS-derived $(\text{OC}/\text{EC})_{\text{pri}}$ in equations (1) and (2), we computed average POC and SOC
concentrations of 2.0 ± 2.4 and $2.8 \pm 3.4 \mu\text{g m}^{-3}$, respectively, suggesting that POC and
SOC contributions to $\text{PM}_{2.5}$ were comparable during our study. The average POC and

330 SOC concentrations were 1.0 ± 1.0 and $2.7 \pm 4.0 \mu\text{g m}^{-3}$, respectively, when transport was
332 from the south/southwest. POC increased to $2.5 \pm 2.7 \mu\text{g m}^{-3}$ and SOC was almost
334 unchanged when the direction of transport was from the north / northeast. Variability in
336 OC was thus mainly due to variability in POC. The sampling locations were in cells
338 classified as being in the outskirts of the city when south/southwesterly transport was
prevalent, but included both outskirts and in-city grids when north/northeasterly transport
was prevalent. The increase in POC during northerly transport regimes could not
therefore be attributed solely to the influence of local primary emissions, since transport
of POC from outside Riyadh was also possible.

The diurnal variation of SOC (Fig. S3) showed a small peak of SOC concentration in the
340 morning from 7-9 am, lagging behind the POC and EC morning peaks by about two hours;
342 this result was not unexpected since photochemical production of SOC will require time
344 for reactions to proceed once precursors have accumulated in the atmosphere. A second
346 small peak in SOC concentration occurred at 14:00 pm, concurrent with ozone formation
(Fig. S4S2) and consistent with the variation in OC/EC ratios discussed in Section 3.3.
348 The diurnal variations of POC and SOC were similar on weekdays and weekends, but the
weekday-to-weekend changes in POC and SOC had opposite trends. The estimated
POC was $2.2 \pm 2.5 \mu\text{g m}^{-3}$ on weekdays and decreased to $1.5 \pm 1.9 \mu\text{g m}^{-3}$ on weekends.
350 The estimated SOC was $2.6 \pm 2.9 \mu\text{g m}^{-3}$ on weekdays and increased by 23% to 3.2 ± 4.5
352 $\mu\text{g m}^{-3}$ on weekends. The elevated SOC during weekends was likely due to regional
production and transport. With regards to spatial variation, POC and SOC were 3.5 ± 2.7
354 and $3.2 \pm 2.9 \mu\text{g m}^{-3}$ in the industrial sites, 2.1 ± 2.6 and $2.6 \pm 3.0 \mu\text{g m}^{-3}$ in the residential
356 sites, and 1.1 ± 1.1 and $2.8 \pm 4.1 \mu\text{g m}^{-3}$ in the outskirts sites, respectively. SOC
358 concentrations were 2.5 times those of POC in the outskirts sites, an expected result
since these latter sites are farther removed from the sources of primary emissions within
the city proper. The results were consistent with the study of von Schneidmesser et al.
(2010) that SOC (i.e., OC that was left unapportioned by a chemical mass balance model)
was estimated to be 30-74% of the total OC in 11 sites in the Middle East, having
climatological conditions similar to those in Riyadh.

3.5 Possible sources of $\text{PM}_{2.5}$ carbonaceous aerosols

360 3.5.1 Correlation between OC, EC and other elemental species

362 As a first step in seeking signatures of sources of carbonaceous aerosol in Riyadh, we
364 conducted an analysis of the correlations between OC or EC and measured elemental
366 species concentrations were obtained for the PM_{10} fraction, which also ~~includes~~ included
the $\text{PM}_{2.5}$. OC and EC were poorly correlated with K, which we interpreted as indicating
a negligible influence of biomass burning on PM. Al, Fe, Mg, Mn, and Ca are found in
crustal soils and in PM samples of windblown dust. EC did not correlate well with these

368 species ($R^2 < 0.35$; not shown). However, OC had a relatively strong correlation with Ca
370 (R^2 of 0.63) (Fig. 8 and Fig. S57) but, similar to EC, a poor correlation with other dust
372 species (not shown). These findings indicated that OC may have shared a source with
374 Ca, but this source ~~is was~~ not likely to be associated with windblown dust. The correlation
376 between SOC and Ca was stronger than that between POC and Ca (Fig. S5S6). The
378 thermo-optical method may have measured CaCO_3 as OC, and the subsequent estimates
380 of SOC separated two sources, one associated with combustion and EC ("primary"), and
another associated with CaCO_3 (and mis-labeled "secondary"). Concentrations of Al and
of other metals (Fe, K, Mg and Mn) were strongly correlated ($R^2 > 0.9$), supporting their
common dust origin (Fig. 8). The correlation between Ca and other dust metal species
(Al, Fe, K, Fe and Mg), however, showed two divergent regimes, suggestive of an
additional Ca-containing source besides dust, that may have shared the same sources
as OC. Therefore, understanding the sources of Ca ~~becomes-became~~ a prerequisite in
understanding the sources of OC.

382 The enrichment factor (EF) is a practical and convenient tool to differentiate natural and
384 anthropogenic sources of metal species (Khodeir et al., 2012; Rushdi, et al., 2013). The
EF can be calculated using the following equation (Taylor, 1964):

$$EF = \frac{(X / C_{ref})_{air}}{(X / C_{ref})_{source}} \quad \text{Eqn 5}$$

386 where X is the measured metal concentration, and C_{ref} is the concentration of the
388 reference metal species. The equation compares the ambient elemental abundance of
390 two species with their source abundance. An EF less than 10 suggests that the sample
392 may come from a natural crustal source and an EF value > 10 indicates possible
394 anthropogenic influence (Biegalski et al., 1998). Al, Fe, and K were all used as reference
396 species to test for robustness of the findings. Fig. S6 shows that, for all three reference
species, the EFs for Al, Fe, K, Mn, Mg, Na and V were calculated to be less than 10,
suggesting a dominant crustal type origin. The EFs of Ni, Zn, Cr, Co, Pb, Li, B, As, Mo,
Cd, and Te were calculated to be larger than 10, suggestive of the influence of
anthropogenic emissions, e.g. traffic emissions, fossil fuel combustion and non-ferrous
metal industries. The EF for Ca was calculated to be ~ 10 , consistent with the idea that it
may have two sources in Riyadh, one natural and one anthropogenic.

398 Cement kilns ~~are~~ have been documented to be important sources of elemental Ca in the
400 atmospheric aerosol (Zhang et al., 2014). Chow et al. (2004) noted an important
402 contribution of $\text{PM}_{2.5}$ POC from cement factories. Hence, contributions from cement
production sources may have led to the good correlation between OC and Ca at the
receptor sites. In the Middle East, another possible anthropogenic source for Ca is from
the desalting and demetalization of crude oil in refineries (Wu et al., 2014); refineries are

Formatted: Font: Italic

404 certainly contributing to the observed OC in Riyadh. A third possibility ~~is-was~~ that the Ca
is crustal in origin, but from a different source region than most of the other sampled dust.
406 Ca enrichment in dusts may vary across the Middle East region (Coz et al., 2010), and
thus the correlation between Ca and other crustal species could diverge depending upon
408 the dust source region. Regardless of dust source region, during transport to Riyadh, as
ambient SOC precursors ~~were~~ oxidized, the products may ~~be-have~~ partitioned to particle
410 surfaces, resulting in simultaneous transport of Ca and OC. Finally, ~~it is important to~~
note that a correlation between Ca and OC may ~~have occurred~~ if calcium carbonate ~~is~~
412 ~~was~~ being sampled and the carbonate detected as OC in the thermal analysis protocol,
as mentioned in the Methods section above. While it ~~is-was~~ not possible to definitively
414 distinguish between these various possibilities based only on EF, the large dust loadings
that were present in nearly all samples suggest that this latter explanation could play a
416 significant role in producing the observed Ca-OC correlations.

3.5.2 CWT analysis for Ca/Al ratio, Pb, OC and EC

418 We used CWT analysis to identify possible source origins for the observed highest values
of Ca/Al ratio, Pb, OC and EC (Fig. 9). The CWT plot for the Ca/Al ratio ~~shows-showed~~
420 that, when this ratio was high in Riyadh PM samples, air masses were most likely to have
passed over regions along the western shoreline of the Persian Gulf, and in particular,
422 the highest ratio was found for air masses passing over the site of a large Saudi Arabian
cement plant (Fig. ~~S7S8~~). This transport pathway ~~is-was~~ thus consistent with the idea that
424 refineries and cement plants may represent anthropogenic sources of Ca. CWT analysis
of Pb ~~shows~~ that high observed concentrations in Riyadh aerosol were associated with
426 transport from Iraq, consistent with the continued usage of leaded fuel in that country
(Shaik et al., 2014). PM₁₀ Pb concentrations were 0.035±0.088 µg m⁻³ in this study, lower
428 than measurements reported for eastern China (0.05 to 0.5 µg m⁻³, Li et al., 2010) and
the greater Cairo area (0.3 µg m⁻³, Safar and Labib, 2010), both locations for which leaded
430 fuel has been phased out of usage², and lower than the U.S ambient concentration
standard for lead (0.15 µg m⁻³ on a ~~3-3~~-month rolling basis; U.S. EPA, 2006). The
432 comparison ~~shows-showed~~ that although Pb may have multiple potential sources in
Riyadh, the concentration levels ~~are-were~~ still below those of concern for human health.
434 Industrial emissions along the Saudi Arabian coast may also contribute some Pb to the
measured aerosol. While high OC concentrations were associated with transport from a
436 similar region of the Persian Gulf as was high Pb, the high-concentration source region
extended further north, encompassing areas with oil fields and refineries and the Baghdad
438 urban region (Fig. ~~S8S9~~). Finally, the CWT plots for OC and EC ~~are-were~~ similar,
suggesting their highest concentrations may be attributed to similar sources, i.e.,
440 refineries, cement factories and urban pollution.

3.6 PMF analysis

442 Three- to five-factor solutions were tested in the PMF model; the three-factor solution was
443 found to have the best solution characteristics (Fig.10). Most of the OC (77%) and EC
444 (90%) together with fractions of the crustal elements appeared in the first factor. We note
445 that 54% of Ca ~~is-was~~ loaded in this factor, as expected since OC was found to be
446 correlated with Ca. No significant crude oil tracers (Ni and V) appeared in the factor,
447 indicating that this factor ~~was~~ not related to oil combustion (Ganor et al., 1988). The CWT
448 analysis suggested that high OC and EC coming from the shoreline of the Persian Gulf
449 may be associated with industrial emissions, including refineries, gas flares in oil fields,
450 and cement production. However, we ~~could~~ not rule out potential contributions to this
451 factor from local vehicular emissions. Therefore, this factor ~~is-was~~ identified as a mixed
452 source: cement industries / gas flares / local vehicles.

453 A key signature in the second factor ~~is-was~~ the significant loading of Pb (98%); it also
454 ~~includes-included~~ some dust species. While leaded fuels have been phased out in Saudi
455 Arabia, as mentioned above, they ~~are-were~~ still in use in Iraq; further, deposition of lead
456 to soils and resuspension is a documented exposure pathway (Laidlaw and Filippelli,
457 2008). CWT analysis also ~~supports-supported~~ a source origin of Pb from Iraq (Fig. 9).
458 Hence Pb may ~~have served~~ as a regional transport tracer in this PMF analysis. However,
459 Pb ~~can-could~~ also be contained in other industrial emissions, including cement
460 manufacturing in the city. The second factor ~~is-was~~ thus identified as leaded fuel
461 combustion from long range transport / industrial emissions.

462 The third factor ~~contains-contained~~ almost all of the V and a large fraction of Ni (>60%),
463 as well as some crustal elements and OC. V and Ni and their ratios have been suggested
464 as markers of emissions from oil fired power plants (Ganor et al., 1988). Barwise (1990)
465 found that the highest V/Ni ratios (>1) among oil samples that they characterized were
466 associated with Abu Dhabi and Suez oils, as contrasted with samples from the North Sea,
467 China, Indonesia, and Australia, reflecting geological differences. The ratio of V/Ni in
468 factor 3 is 3.5, consistent with the Arabian Gulf source of oil in this region. Dust species
469 and some OC and EC ~~are-were~~ also associated with this factor, which we therefore
470 identified as oil combustion.

471 Fig. 11 shows the source contribution to OC and EC from these three factors in individual
472 samples. On average, the OC concentration was dominated by the mixed source (factor
473 1) ($3.8 \mu\text{g m}^{-3}$, 77%), followed by leaded fuel from long range transport ($0.8 \mu\text{g m}^{-3}$, 27%)
474 and oil combustion ($0.3 \mu\text{g m}^{-3}$, 6%). The contribution of the mixed source ranged from
475 37% in May ($0.7 \mu\text{g m}^{-3}$) to ~~9795%~~ in September (~~7.66.7~~ $\mu\text{g m}^{-3}$). ~~In some May samples,~~
476 ~~mixed source contribution was negligible while the leaded fuel from long range transport~~
477 ~~was dominant.~~ The EC concentration was also mainly attributed to the mixed source (1.9
478 $\mu\text{g m}^{-3}$, 92%). ~~In some May samples, the mixed source contribution was negligible, as the~~
479 ~~source tracer, EC, was only 0.1-0.4 $\mu\text{g m}^{-3}$, about one order of magnitude lower than that~~

Formatted: Superscript

480 [in other periods. The tracer analysis suggested that long-range transport was dominant](#)
481 [for those samples.](#)

482 **4. Conclusions**

483 To our knowledge, this study represents the first reported long-term and spatially resolved
484 hourly measurements of ambient OC and EC concentrations for Riyadh, Saudi Arabia,
485 along with supporting measurements that enable a source apportionment of these
486 important aerosol species. We found that OC and EC average concentrations were
487 comparable to other reported measurements in Middle Eastern cities, and diurnal and
488 weekly variations indicated a clear influence from local emissions. However, OC and EC
489 concentrations varied with air mass source origin, indicative of not only variations across
490 Riyadh and its outskirts, but also of the influence of regional sources on carbonaceous
491 aerosol concentrations. ~~Due to the limited sample size, this study could not separately~~
492 ~~quantify the local and regional source contributions for OC and EC.~~ About half of the
493 measured OC was attributed to secondary formation, and positive matrix factorization
494 suggested that EC and OC were mainly attributed to a mixed source category comprising
495 cement industries, gas flaring activities, and local vehicles.

496 Measurement of OC and EC via the online thermo-optical technique was found to be
497 challenging in the dusty environment encountered year-round in Riyadh. Our dataset
498 required correction via a hand analysis, as reported in the supplementary materials, as
499 the automated split method implemented by the manufacturer frequently failed for our
500 samples. The lack of a separate independent carbonate analysis, however, means that
501 our reported OC concentrations may be biased high, as also suggested by the strong
502 correlation between OC and Ca. However, the correlation between OC and Ca may also
503 suggest co-emission of OC and its precursors with metal Ca from desalting and
504 demetalization processes in refineries; co-emission of Ca and OC from cement plants; or
505 condensation of OC on Ca-rich dust during long-range transport. In future studies of
506 ambient aerosol OC concentrations in dusty environments via online thermo-optical
507 techniques, additional observations or different measurement protocols are needed to
508 separate the contributions of carbonates to the measured OC and EC concentrations.
509 With such added information, the implied sources of Ca and OC can be further
510 investigated and their potential contributions to observed OC quantified.

512 **Appendix A: Correction method for OC/EC splits in data from the Sunset semi-** 513 **continuous analyzer**

514 Laser response and temperature for individual blanks were well correlated,
515 suggesting that the influence of temperature on laser response may indirectly affect the
516 EC/OC split points (Figure A.1). This phenomenon has been pointed out previously, and

518 Versions RT-Calc 114 and newer of the Sunset instrument analysis software introduced
a laser correction factor to counteract the influence of temperature on the laser signal.
520 This correction factor is calculated in each cycle from the variation in the laser signal when
the analysis enters the methane calculation stage (Jung et al., 2011). However, it was
522 obvious that this correction approach did not work well for the Riyadh samples, since
many returned EC/TC=0, the case when the initial reflectance is not recovered in the
analysis. A revised method of finding the point of return to the original laser signal, and
524 thus determining the POC and EC contributions, was therefore proposed for this study
and used to correct the dataset.

526 The relationship for the Riyadh samples between laser response and temperature
during the calibration phase of the CH₄ + O₂ injection was used to develop a corrected
528 split point, assuming that only refractory material is present in this phase, and the effects
of this refractory material on the laser response to temperature variations could be
530 isolated and then applied during the other analysis phases. A correlation between laser
response and temperature in the calibration phase was derived using linear and quadratic
532 functions. The derived parameters from the two functions were applied in the following
equations to recompute a corrected laser signal for each analysis, instead of the laser
534 correction factor automatically generated by the Sunset program:

$$536 \quad \text{Signal}_{new} = \text{Signal}_{original} + a (\text{Temp}_{initial}^2 - \text{Temp}_{original}^2) \\ + b (\text{Temp}_{initial} - \text{Temp}_{original}) \quad (\text{A.1})$$

$$538 \quad \text{Signal}_{new} = \text{Signal}_{original} + c (\text{Temp}_{initial} - \text{Temp}_{original}) \quad (\text{A.2})$$

540 where $\text{Signal}_{original}$ ~~represents-represented~~ the original laser signal, Signal_{new} ~~represents~~
542 ~~represented~~ the signal after correction to the initial temperature, $\text{Temp}_{initial}$ ~~represents~~
~~represented~~ the temperature at the initial condition when each analysis ~~begins~~~~began~~, and
544 $\text{Temp}_{original}$ ~~represents-represented~~ the original temperature for each analysis; a and b in
Eq. (A.1) ~~are-were~~ derived from the quadratic equation for each analysis, and c in Eq.
546 (A.2) was derived from a linear fit.

548 Since refractory residues accumulated on the filter during the measurement period,
the derived correlation between laser response and temperature varied sample by sample.
The equations to derive the corrected laser signal were, therefore, applied individually to
550 each sample. In the blank sample, the quadratic-function-generated laser signal was
smoother than the linear-function-generated one, especially during the calibration phase

552 of the CH₄ + O₂ injection (Figure A.2a). The relationship between temperature and laser
554 signal for the newly replaced filter tended to be closer to linear, while the signal for the
aged filter with residue accumulation showed a better fit using a quadratic equation. A
quadratic equation was therefore selected to correct the laser signal for the entire dataset.
556 The new split points were then set to where the corrected laser signal rebounded to its
value just before OC pyrolyzed and the laser signal decreased due to pyrolyzed organic
558 carbon formation. The method worked for both incorrect split-point cases, bringing the
split point back to the He + O₂ phase as expected and leading to more reasonable EC/OC
560 split points, i.e., neither at the end of the analysis nor in the pre-oxygen analysis phase.
It is noted that although the quadratic equation correction produced a better laser signal
562 for purposes of the carbon analyses, this correction does not work perfectly in the low
temperature He phase, where the corrected laser signals exhibited unexpected
564 increases. However, this shortcoming does not substantially influence the accuracy of
the correction during subsequent carbon evolution. We note that premature evolution of
566 EC, leading to an increasing laser signal in the inert environment due to the existence of
refractory metal oxides, was observed in the studies of Wang et al. (2010) and Bladt et
568 al. (2012). The increases in the corrected laser signal during the He stage in this study
may be partially due to the same cause, as Riyadh samples contained abundant metal
570 oxides.

572

Acknowledgments

574 The authors gratefully acknowledge the financial support of King Abdulaziz City for
Science and Technology (KACST) under grant number [32-594](#) and the NOAA Air
576 Resources Laboratory (ARL) for the provision of the HYSPLIT transport and dispersion
model and the READY website (<http://www.ready.noaa.gov>) used in this publication.

References

Abdeen, Z., Qasrawi, R., Heo, J., Wu, B., Shpund, J., Vanger, A., Sharf, G., Moise, T.,
580 Brenner, S., Nassar, K., Saleh, R., Al-Mahasneh, Q.M., Sarnat, J.A., and Schauer, J.J.:
Spatial and Temporal Variation in Fine Particulate Matter Mass and Chemical
582 Composition: The Middle East Consortium for Aerosol Research Study, Scientific World
J., 878704, 2014.

584 Al-Dabbous, A.N., and Kumar, P.: Source apportionment of airborne nanoparticles in a
Middle Eastern city using positive matrix factorization, Environ. Sci.: Processes Impacts,
586 17, 802-812, DOI: 10.1039/C5EM00027K, 2015.

588 Alharbi, B., Shareef, M.M., and Husain, T.: Study of chemical characteristics of particulate
matter concentrations in Riyadh, Saudi Arabia, *Atmos. Pollut. Res.*, 6, 88-98, 2015.

590 Ashbaugh, L.L., Malm, W.C., and Sadeh, W.Z.: A residence time probability analysis of
sulfur concentrations at Grand Canyon National Park, *Atmos. Environ.*, 19, 1263-
1270, 1985.

592 Bae, M.-S., Schauer, J. J., DeMinter, J. T., and Turner, J. R.: Hourly and Daily Patterns
of Particle-Phase Organic and Elemental Carbon Concentrations in the Urban
594 Atmosphere, *J. Air Waste Manag. Assoc.*, 54, 823-833, DOI:10.1080/10473289.2004.10470957, 2004.

596 Barrett, T. E. and Sheesley, R. J.: Urban impacts on regional carbonaceous aerosols:
case study in central Texas, *J. Air Waste Manag. Assoc.*, 64, 917-26, 2014.

598 Barwise, A.J.G.: Role of Nickel and Vanadium in Petroleum Classification, *Energy Fuels*,
4, 647-652, DOI: 10.1021/ef00024a005, 1990.

600 [Batmunkh, T., Lee, K., Kim, Y. J., Bae, M.-S., Maskey, S., Park, K.: Optical and thermal](#)
602 [characteristics of carbonaceous aerosols measured at an urban site in Gwangju, Korea,](#)
[in the winter of 2011, *J. Air & Waste Manage Association*, 66, 151-163, DOI:](#)
[10.1080/10962247.2015.1101031, 2016.](#)

604 Biegalski S.R., Landsberger S, and Hoff R.M.: Source-receptor modeling using trace
metals in aerosols collected at three rural Canadian Great lakes Sampling Stations., *J. Air*
606 *Waste Manage. Assoc.*, 48, 227–37, 1998.

608 Bond, T. C., Doherty, S. J., Fahey, D. W., Forster, P. M., Berntsen, T., DeAngelo, B. J.,
Flanner, M. G., Ghan, S., Kärcher, B., Koch, D., Kinne, S., Kondo, Y., Quinn, P. K.,
610 Sarofim, M. C., Schultz, M. G., Schulz, M., Venkataraman, C., Zhang, H., Zhang, S.,
Bellouin, N., Guttikunda, S. K., Hopke, P. K., Jacobson, M. Z., Kaiser, J. W., Klimont, Z.,
Lohmann, U., Schwarz, J. P., Shindell, D., Storelvmo, T., Warren, S. G. and Zender, C.
612 S.: Bounding the role of black carbon in the climate system: A scientific assessment, *J.*
Geophys. Res. Atmos., 118, 5380–5552, doi:10.1002/jgrd.50171, 2013.

614 Chow, J. C., Watson, J. G., Kuhns, H., Etyemezian, V., Lowenthal, D. H., Crow, D., Kohl,
S. D., Engelbrecht, J. P., and Green, M. C.: Source profiles for industrial, mobile, and
616 area sources in the Big Bend Regional Aerosol Visibility and Observational study,
Chemosphere, 54, 185-208, 2004.

618 Chow, J. C., Watson, J. G., Lowenthal, D.H., Chen, L.-W. Antony, and Motallebi, N.:
PM2.5 source profiles for black and organic carbon emission inventories, *Atmos. Environ.*,
620 45, 5407-5415, 2011.

622 Coz, E., Gómez-Moreno, F.J., Casuccio, G.S., and Artíñano, B.: Variations on
morphology and elemental composition of mineral dust particles from local, regional, and
624 long-range transport meteorological scenarios, *J. Geophys. Res.*, 115, D12204,
doi:10.1029/2009JD012796, 2010.

626 Draxler, R.R. and Rolph, G.D. HYSPLIT (HYbrid Single-Particle Lagrangian Integrated
Trajectory) Model access via NOAA ARL READY Website
(<http://www.arl.noaa.gov/HYSPLIT.php>). NOAA Air Resources Laboratory, College Park,
628 MD.

630 Engelbrecht, J. P., McDonald, E. V., Gillies, J. A. Jayanty, R. K. M., Casuccio, G., and
Gertler, A. W.: Characterizing Mineral Dusts and Other Aerosols from the Middle East –
Part 2: Grab Samples and Re-Suspensions, *Inhal. Toxicol.*, 21, 327-36, doi:
632 10.1080/08958370802464299, 2009.

634 Ganor, E., Altshuler, S., Foner, H.A. Brenner, S., and Gabbay, J.: Vanadium and nickel
in dustfall as indicators of power plant pollution, *Water Air Soil Pollut.*, 42,241-252,
doi:10.1007/BF00279270, 1988.

636 Genberg, J., Hyder, M., Stenström, K., Bergström, R., Simpson, D., Fors, E.O., Jönsson,
J.Å., and Swietlicki, E.: Source apportionment of carbonaceous aerosol in southern
638 Swede, *Atmos. Chem., Phys.*, 11, 11387-11400, doi:10.5194/acp-11-11387-2011, 2011.

640 Gentner, D. R., Issacman, G., Worton, D. R., Chan, A. W. H., Dallmann, T. R., Davis, L.,
Liu, S., Day, D. A., Russell, L. M., Wilson, K. R., Weber, R., Guha, a., Harley, R. A., and
642 Goldstein, A. H.: Elucidating secondary organic aerosol from diesel and gasoline vehicles
through detailed characterization of organic carbon emissions, *Proc. Natl. Acad. Sci.*
U.S.A., 109, 18318-18323, doi: 10.1073/pnas.1212272109, 2012.

644 Ginoux, P., Prospero, J.M., Gill, T.E., Hsu, N.C., and Zhao, M.,: Global-scale attribution
of anthropogenic and natural dust sources and their emission rates based on MODIS
646 Deep Blue aerosol products, *Rev. Geophys.*, 50, RG3005, doi:10.1029/2012RG000388,
2012.

648 Givhechi, R., Arhami, M., and Tajrishy, M.: Contribution of the Middle Eastern dust source
areas to PM10 levels in urban receptors: Case study of Tehran, Iran, *Atmos. Environ.*, 75,
650 287-295, 2013.

652 Gray, H. A., Cass, G. R., Huntzicker, J. J., Heyerdahl, E. K., and Rau, J. A.:
Characteristics of atmospheric organic and elemental carbon particle concentrations in
Los-Angeles, *Environ. Sci. Technol.*, 20, 580–589, DOI: 10.1021/es00148a006, 1986.

- 654 Grivas, G., Cheristanidis, S., and Chaloulakou, A.: Elemental and organic carbon in the
656 urban environment of Athens. Seasonal and diurnal variations and estimates of
secondary organic carbon, *Sci Total Environ*, 414, 535–545, 2012.
- 658 Han, J.S., Moon, K.J., Ryu, S. Y., Kim, Y. J., and Perry, K. D.: Source estimation of
660 anthropogenic aerosols collected by a DRUM sampler during spring of 2002 at Gosan,
Korea, *Atmos. Environ.*, 39, 3113-3125, 2005.
- Harrison, R.M., Jones, A.M., Gietl, J., Yin, J., and Green, D.C.: Estimation of the
662 Contributions of Brake Dust, Tire Wear, and Resuspension to Nonexhaust Traffic
Particles Derived from Atmospheric Measurements, *Environ. Sci. Technol.*, 46, 6523-
664 6529, DOI: 10.1021/es300894r, 2012.
- Heal, M.R. and Hammonds, M.D.: Insights into the Composition and Sources of Rural,
666 Urban and Roadside Carbonaceous PM₁₀, *Environ. Sci. Technol.*, 48, 8995-9003, DOI:
10.1021/es500871k, 2014.
- 668 Ho, K. F., Lee, S. C., Cao, J. J., Li, Y. S., Chow, J. C., Watson, J. G., and Fung, K.:
670 Variability of organic and elemental carbon, water soluble organic carbon, and isotopes
in Hong Kong, *Atmos. Chem. Phys.*, 6, 4569-4576, doi:10.5194/acp-6-4569-2006, 2006.
- Hong, Y.C., Pan, X.C., Kim, S.Y., Park, K., Park, E.J., Jin, X., Yi, S.M., Kim, Y.H., Park,
672 C.H., Song, S. and Kim, H.: Asian Dust Storm and Pulmonary Function of School Children
in Seoul, *Sci. Total Environ*. 408, 754– 759, 2010.
- 674 Hu, W.W., Hu, M., Deng, Z.Q., Xiao, R., Kondo, Y., Takegawa, N., Zhao, Y.J., Guo, S.,
676 and Zhang, Y.H.: The characteristics and origins of carbonaceous aerosol at a rural site
of PRD in summer of 2006, *Atmos. Chem. Phys*, 12, 1811-1822, doi:10.5194/acp-12-
1811-2012, 2012.
- 678 Huang, X.H.H., Bian, Q.J., Louie, P.K.K., and Yu, J.Z.: Contributions of vehicular
carbonaceous aerosols to PM_{2.5} in a roadside environment in Hong Kong, *Atmospheric
680 Chemistry and Physics*, *Atmos. Chem. Phys.*, 14, 9279–9293, doi:10.5194/acp-14-9279-
[2014](#), 2014a.
- 682 Huang, X. H. H., Bian, Q., Ng, W. M., Louie, P. K. K., Yu, J. Z., Characterization of PM_{2.5}
Major Components and Source Investigation in Suburban Hong Kong: A One Year
684 Monitoring [Study. Aerosol](#) *Air Qual. Res.*, 14, 237-250, doi: 10.4209/aaqr.2013.01.0020,
2014b.
- 686 Jacobson, M.C., Hansson, H.-C., Noone, K.J., and Charlson, R.J.: Organic atmospheric
688 aerosols: Review and state of the science, *Rev. Geophys.*, 38, 267-294, DOI:
10.1029/1998RG000045, 2000.

690 Jeong, C. H., Hopke, P. K., Kim, E., and Lee, D. W.: The comparison between
thermaleoptical transmittance elemental carbon and Aethalometer black carbon
measured at multiple monitoring sites, *Atmos. Environ.*, 38, 5193–5204, 2004.

692 Jimenez, J. L., Canagaratna, M. R., Donahue, N. M., Prevot, A. S. H., Zhang, Q., Kroll, J.
H., DeCarlo, P. F., Allan, J. D., Coe, H., Ng, N. L., Aiken, A. C., Docherty, K. S., Ulbrich,
694 I. M., Grieshop, A. P., Robinson, A. L., Duplissy, J., Smith, J. D., Wilson, K. R., Lanz, V.
A., Hueglin, C., Sun, Y. L., Tian, J., Laaksonen, A., Raatikainen, T., Rautiainen, J.,
696 Vaattovaara, P., Ehn, M., Kulmala, M., Tomlinson, J. M., Collins, D. R., Cubison, D. R.,
Dunlea, E. J., Huffman, J. A., Onasch, T. B., Alfarra, M. R., Williams, P. I., Bower, K.,
698 Kondo, Y., Schneider, J., Drewnick, F., Borrmann, S., Weimer, S., Demerjian, K., Salcedo,
D., Cottrell, L., Griffin, R., Takami, A., Miyoshi, T., Hatakeyama, S., Shimono, A., Sun, J.
700 Y., Zhang, Y. M., Dzepina, K., Kimmel, J. R., Sueper, D., Jayne, J. T., Herndon, S. C.,
Trimborn, A. M., Williams, L. R., Wood, E. C., Middlebrook, A. M., Kolb, C. E.,
702 Baltensperger, U., and Worsnop, D. R.: Evolution of organic aerosols in the atmosphere,
Science, 326, 1525–1529, doi:10.1126/science.1180353, 2009.

704 Jung, J., Kim, Y.J., Lee, K.Y., Kawamura, K., Hu, M., and Kondo, Y.: The effects of
706 accumulated refractory particles and the peak inert mode temperature on semi-
continuous organic carbon and elemental carbon measurements during the CAREBeijing
2006 campaign, *Atmos. Environ.*, 45, 7192-7200, 2011.

708 Kanakidou, M., Seinfeld, J., Pandis, S., Barnes, I., Dentener, F., Facchini, M., Van
Dingenen, R., Ervens, B., Nenes, A., and Nielsen, C.: Organic aerosol and global climate
710 modelling: a review, *Atmos. Chem. Phys.*, 5, 1053-1123, doi:10.5194/acp-5-1053-2005,
2005.

712 Karanasiou, A. A., Siskos, P.A., and Eleftheriadis, K.: Assessment of source
apportionment by positive matrix factorization analysis on fine and coarse urban aerosol
714 size fractions, *Atmos. Environ.*, 43, 3385-3395, 2009.

Karanasiou, A., Diapouli, E., Cavalli, F., Eleftheriadis, K., Viana, M., Alastuey, A., Querol,
716 X., and Reche, C.: On the quantification of atmospheric carbonate carbon by
thermal/optical analysis protocols, *Atmos. Meas. Tech.*, 4, 2409-2419, doi:10.5194/amt-
718 4-2409-2011, 2011.

Khan, M. B., Masiol, M., Formenton, G., Gilio, A. D., de Gennaro, G., Agostinelli, C., and
720 Pavoni, B.: Carbonaceous PM_{2.5} and secondary organic aerosol across the Veneto
Region (NE Italy), *Sci. Total Environ.*, 542A, 172-181, 2016.

722 Khodeir, M., Shamy, M., Alghamdi, M., Zhong, M., Sun, H., Costa, M., Chen, L.-C., and
Maciejczyk, P.: Source Apportionment and Elemental Composition of PM_{2.5} and PM₁₀
724 in Jeddah City, Saudi Arabia, *Atmos. Pollut. Res.*, 3, 331-340, 2012.

- 726 Laidlaw, M. A. S. and Fillpelli, G. M.: Resuspension of urban soils as a persistent source
of lead poisoning in children: A review and new directions, *Appl. Geochem.*, 23, 2021-
2039, 2008.
- 728 Lee, H.J., Gent, J.F., Leaderer, B.P., and Koutrakis, P.: Spatial and temporal variability
of fine particle composition and source types in five cities of Connecticut and
730 Massachusetts, *Sci. Total Environ*, 409, 2133-2142, 2011.
- Li, C., Wen, T., Li, Z., Dickerson, R. R., Yang, Y., Zhao, Y., Wang, Y., and Tsay, S.-C.:
732 Concentrations and origins of atmospheric lead and other trace species at a rural site in
northern China, *J. Geophys. Res.*, 115, D00K23, doi:10.1029/2009JD013639, 2010.
- 734 Lim, H.-J. and Turpin, B. J.: Origins of Primary and Secondary Organic Aerosol in Atlanta:
Results of Time-Resolved Measurements during the Atlanta Supersite Experiment,
736 *Environ. Sci. Technol.*, 36, 4489-4496, DOI: 10.1021/es0206487, 2002.
- Lippmann, M., Ito, K., Hwang, J.-S., Maciejczyk, P., and Chen, L.-C.: Cardiovascular
738 Effects of Nickel in Ambient Air, *Environ. Health Perspect.*, 114, 1662-1669, doi:
10.1289/ehp.9150, 2006.
- 740 Lough, G. C., Schauer, J. J., and Lawson, D. R.: Day of week trends in carbonaceous
aerosol composition in the urban atmosphere, *Atmos. Environ.*, 40, 4137-4149, 2006.
- 742 Millet, D.B., Donahue, N.M., Pandis, S.N., Polidori, A., Stanier, C.O., Turpin, B.J., and
Goldstein, A.H.: Atmospheric volatile organic compound measurements during the
744 Pittsburgh Air Quality Study: Results, interpretation, and quantification of primary and
secondary contributions, *J. Geophys. Res.*, 110, D07S07, doi:10.1029/2004JD004601,
746 2005.
- Motallebi, N., Tran, H., Croes, B. E., and Larsen, L. C.: Day-of-week patterns of particulate
748 matter and its chemical components at selected sites in California, *J. Air Waste Manag.*
Assoc., 53, 876-88, 2003.
- 750 Norris, G., Duvall, R., Brown, S., Bai S.: EPA Positive Matrix Factorization (PMF) 5.0
Fundamentals and User Guide, available at:
752 https://www.epa.gov/sites/production/files/2015-02/documents/pmf_5.0_user_guide.pdf,
[2014](https://www.epa.gov/sites/production/files/2015-02/documents/pmf_5.0_user_guide.pdf).
- 754 Ondov, J. M., Buckley, T. J., Hopke, P. K., Ogulei, D., Parlange, M. B., Rogge, W. F.,
Squibb, K. S., Johnston, M. V., and Wexler, A. S.: Baltimore supersite: highly time- and
756 size- resolved concentrations of urban PM_{2.5} and its constituents for resolution of
sources and immune response, *Atmos. Environ.*, 40, 224-237, 2006.

- 758 Panda, S., Sharma, S.K., Mahapatra, P. S., Panda, U., Rath, S., Mahapatra, M., Mandal,
760 T. K., and Das, T.: Organic and elemental carbon variation in PM_{2.5} over megacity Delhi
and Bhubaneswar, a semi-urban coastal site in India, *Nat. Hazards*, 80, 1709-1728, 2016.
- Peltier, R.E., and Lippmann M.: Residual oil combustion: 2. Distributions of airborne nickel
762 and vanadium within New York City, *J. Expo. Sci. Environ. Epidemiol.*, 20, 342-50, doi:
10.1038/jes.2009.28, 2010.
- 764 Polidori, A., Turpin, B.J., Lim, H-J., Cabada, J.C., Subramanina, R., Pandis, S.N, and
766 Robinson, A. L.: Local and regional secondary organic aerosol: insights from a year of
semi-continuous carbon measurements at Pittsburgh, *Aerosol Sci. .Tech.*, 40, 861-872,
DOI: 10.1080/02786820600754649, 2007.
- 768 Polissar, A.V., P.K. Hopke, W.C. Malm, and Sisler, J. F.: Atmospheric Aerosol over Alaska:
770 2. Elemental Composition and Sources, *J. Geophys. Res.* 103, 19045-19057, DOI:
10.1029/98JD01212, 1998.
- Querol, X., Viana, M., Alastuey, A., Amato, F., Moreno, T., Castillo, S., Pey, J., de la Rosa,
772 J., Artinano, B. Salvador, P., Garcia Dos Santos, S., Fernandez-Patier, R., Moreno-Grau,
s., Negral, L., Minguillon, M. C., Monfort, E., gil, J.I., Inza, A., Ortega, L.A., Santamaria,
774 J.M., and Zabalza, J.: Source origin of trace elements in PM from regional background,
urban and industrial sites of Spain, *Atmos. Environ.*, 41, 7219-7231., 2007.
- 776 Ramanathan, V. and Carmichael., G.: Global and regional climate changes due to black
carbon, *Nat. Geosci.*, 1, 221-227, doi:10.1038/ngeo156, 2008.
- 778 Reff, A., Eberly, S. I., and Bhave, P. V.: Receptor modeling of ambient particulate matter
780 data using positive matrix factorization: review of existing methods, *J. Air Waste Manag.*,
57, 146-154, 2007.
- Robinson, A. L., Donahue, N. M., Shrivastava, M. K., Weikamp, E. A., Sage, A. M.,
782 Greishop, A. P., Lane, T. E., Pierce, J. R. and Pandis, S. N.: Rethinking Organic Aerosols:
Semivolatile Emissions and Photochemical Aging, *Science*, 315, 1259-1262, DOI:
784 10.1126/science.1133061, 2007.
- Rolph, G.D.: Real-time Environmental Applications and Display sYstem (READY)
786 Website (<http://www.ready.noaa.gov>). NOAA Air Resources Laboratory, College Park,
MD, 2016.
- 788 Rushdi, A.I., Al-Mutlaq, K.F., Al-Otaibi, M., El-Mubarak, A.H., and Simoneit, B.R.T: Air
790 quality and elemental enrichment factors of aerosol particulate matter in Riyadh City,
Saudi Arabia, *Arab. J. Geosc.*, 6, 585-599, DOI: 10.1007/s12517-011-0357-9, 2013.

792 Saarikoski, S., Timonen, H., Saarnio, K, Aurela, M., Järvi, L., Keronen, P., Kerminen, V.-
M., and Hillamo, R.: Sources of organic carbon in fine particulate matter in northern
794 European urban air, *Atmos. Chem. Phys.*, 8, 6281-6295, doi:10.5194/acp-8-6281-2008,
2008

796 Safar, Z. S. and Labib, M. W.: Assessment of particulate matter and lead levels in the
Greater Cairo for the period 1998-2007, *J. Adv. Res.*, 1, 53-63, 2010.

798 Satsangi, A., Pachauri, T., Singla, V., Lakhani, A., and Kumari, K. M.: Organic and
elemental carbon aerosols at a suburban site, *Atmos. Res.*, 113, 13–21, 2012.

800 Schwarz, J., Chi, X., Maenhaut, W., Civiš, M., Hovorka, J., and Smolík, J.: Elemental and
organic carbon in atmospheric aerosols at downtown and suburban sites in Prague.
Atmos. Res., 90, 287-302., 2008.

802 Shaik, A.P., Sultana, S. A., and Alsaeed, A. H.: Lead Exposure: A Summary of Global
Studies and the Need for New Studies from Saudi Arabia, *Dis. Markers*, 2014, 415160,
804 <http://dx.doi.org/10.1155/2014/415160>, 2014.

806 [Snyder, D. C., Rutter, A. P., Worley, C., Olson, M., Plourde, A., Bader, R. C., Dallmann,
T., Schauer, J. J.: Spatial variability of carbonaceous aerosols and associated source
808 tracers in two cities in the Midwestern United States, *Atmos. Environ.*, 44, 1597-1608,
2010.](#)

810 Stein, A.F., Draxler, R.R, Rolph, G.D., Stunder, B.J.B., Cohen, M.D., and Ngan, F.:
NOAA's HYSPLIT atmospheric transport and dispersion modeling system, *Bull. Amer.
Meteor. Soc.*, **96**, 2059-2077, 2015.

812 Taylor, S. R.: Abundance of chemical elements in the continental crust: A new table,
Geochim. Cosmochim. Acta., 28, 1273-1285, 1964.

814 Tsiouri, V., Kakosimos, K. E., and Kumar, P.: Concentrations, sources and exposure risks
associated with particulate matter in the Middle East Area – a review, *Air. Qual. Atmos.
816 Health*, 8, 67-80, DOI: 10.1007/s11869-014-0277-4, 2015.

818 Turpin, B.J., and Huntzicker, J. J.: Identification of secondary organic aerosol episodes
and quantification of primary and secondary organic aerosol concentrations during
SCAQS, *Atmos. Environ.*, 29, 3527-3544, 1995.

820 U.S. EPA. Air Quality Criteria for Lead (Final Report, 2006). U.S. Environmental
Protection Agency, Washington, DC, EPA/600/R-05/144aF-bF, 2006.

822 Viana, M., Kuhlbusch, T.A., Querol, X., Alastuey, A., Harrison, R. M., Hopke, R. M.,
Winiwarer, P. K., Vallius, M., Szidat, S., Prevot, A. S. H., Hueglin, C., Bloemen, H.,
824 Wahlin, P., Vecchi, R., Miranda, A. I., Kasper-Giebl, A., Maenhaut, W., and Hitzenberger,

826 R.: Source apportionment of particulate matter in Europe: a review of methods and
results, *J. Aerosol Sci.*, 39, 827-849, 2008.

828 Vodička, P., Scharz, J., and Ždímal, V., Analysis of one year's OC/EC data at a Prague
suburban site with 2h time resolution, *Atmos. Environ.*, 77,865-872, 2013.

830 [von Schneidmesser, E., Zhou, J., Stone, E. A., Schauer, J. J., Qasrawi, R., Abdeen, Z.,
Shpund, J., Vanger, A., Sharf, G., Moise, T., Brenner, S., Nassar, K., Saleh, R., Al-
Mahasneh, Q. M., Sarnat, J.A.: Seasonal and spatial trends in the sources of fine particle
832 organic carbon in Israel, Jordan, and Palestine, *Atmos. Environ.*, 44, 3669-3678, 2010.](#)

834 Wang, M., Xu, B., Zhao, H., Cao, J, Joswiak, D., Wu, G., and Lin, S.: The influence of
dust on quantitative measurements of black carbon in ice and snow when using a thermal
optical method, *Aerosol Sci. Tech.*, 46, 60-69, DOI: 10.1080/02786826.2011.605815,
836 2012.

838 Weinhold, B.: Global Bang for the Buck Cutting Black Carbon and Methane Benefits Both
Health and Climate, *Environ. Health Perspect.*, 120, A245-A245., doi: 10.1289/ehp.120-
a245b, 2012.

840 Wu, B., Zhu, J., and Li, X. : Distribution of calcium, nickel, iron, and manganese in super-
heavy oil from Liaohe Oilfield, China, *Pet. Sci.*, 11, 590-595, DOI: 10.1007/s12182-014-
842 0376-8, 2014.

844 Wu C. and Yu J.Z.: Determination of primary combustion source organic carbon-to-
elemental carbon (OC / EC) ratio using ambient OC and EC measurements: secondary
OC-EC correlation minimization method, *Atmos. Chem. Phys.*, 16, 5453-5465,
846 doi:10.5194/acp-16-5453-2016, 2016.

848 Yu, L., Wang, G., Zhang, R., Zhang, Song, Y., Wu, B., Li, X., An, K., and Chu, J.:
Characterization and Source Apportionment of PM_{2.5} in an Urban Environment in Beijing,
Aerosol Air Qual. Res., 13, 574-583, doi: 10.4209/aaqr.2012.07.0192, 2013.

850 Zhang, Q., Jimenez, J.L., Canagaratna, M.R., Allan, J.D., Coe, H., Ulbrich, I., Alfarra,
M.R., Takami, A., Middlebrook, A.M., Sun, Y.L., Dzepina, K., Dunlea, E., Docherty, K.,
852 DeCarlo, P.F., Salcedo, D., Onasch, T., Jayne, J.T., Miyoshi, T., Shimojo, A.,
Hatakeyama, S., Takegawa, N., Kondo, Y., Schneider, J., Drewnick, F., Borrmann, S.,
854 Weimer, S., Demerjian, K., Williams, P., Bower, K., Bahreini, R., Cottrell, L., Griffin, R.J.,
Rautiainen, J., Sun, J.Y., Zhang, Y.M. and Worsnop, D.R.: Ubiquity and Dominance of
856 Oxygenated Species in Organic Aerosols in Anthropogenically-Influenced Northern
Hemisphere Midlatitudes, *Geophys. Res. Lett.*, 34, L13801, doi: 10.1092/2007GL029979,
858 2007.

- 860 Zhang, Q., Shen, Z, Cao, J., Ho, K.F., Zhang, R., Bie, Z., Chang, H., and Liu, S.: Chemical
profiles of urban fugitive dust over Xi'an in the south margin of the Loess Plateau, China,
Atmos. Pollut. Res., 5, 421-430, 2014.
- 862 Zhao, P, Dong, F, Yang, Y., He, D., Zhao, X., Zhang, W., Yao, Q., and Liu, H.:
Characteristics of carbonaceous aerosol in the region of Beijing, Tianjin, and Hebei, China,
864 Atmos. Environ., 71, 389-398, 2013.

Table 1 Comparison of OC and EC concentrations ($\mu\text{g m}^{-3}$) measured in the different cities urban areas world-wide.

City	Duration	EC	OC	EC	OC	References
		Conc. ($\mu\text{g m}^{-3}$)		S.D. ($\mu\text{g m}^{-3}$)		
Athens, Greece	Jan to Aug, 2003	2.2	6.8			Grivas et al., 2012
Riesel, TX, US	May, 2011 to Aug, 2012	0.18	2.67	0.09	1.62	Barrett and Sheesley, 2014
Beijing, China	Selective days in four seasons from 2009 to 2010	6.3	18.2	2.9	13.8	Zhao et al., 2013
Urban, Hong Kong	Nov, 2000 to Feb, 2001 and Jun, 2001 to Aug, 2001	5.71	10.12	0.89	1.92	Ho et al., 2006
Suburban, Hong Kong	Mar, 2011 to Feb, 2012	0.86	4.70	0.53	2.87	Huang et al., 2014b
Middle east (11 sampling sites in Palestine, Jordan and Israel)	Jan to Dec, 2007	2.1	5.3	2.2	4.0	Abdeen, et al., 2014
Veneto, Italy	Apr 2012 to Feb 2013	1.3	5.5			Khan et al., 2016
Delhi, India	Dec 20, 2012 to Feb 26, 2013	12.04	16.46	4.43	6.61	Panda et al., 2016
Riyadh, Saudi Arabia	Apr to Sep, 2012	2.13	4.76	2.52	4.4	this study

City	Duration	EC	OC	EC	OC	References
		Conc. ($\mu\text{g m}^{-3}$)		S.D. ($\mu\text{g m}^{-3}$)		
Athens, Greece	Jan to Aug, 2003	2.2	6.8			Grivas et al., 2012
Gwangju, Korea	Winter of 2011	1.7	5.0	0.9	2.5	Batmunkh et al., 2016
Cleveland, US	Jul, 2007 and Jan, 2008	0.33	3.1	0.01	0.78	Snyder et al., 2010
Detroit, US		0.35	3.54	0.01	0.86	
Beijing, China	Selective days in four seasons from 2009 to 2010	6.3	18.2	2.9	13.8	Zhao et al., 2013
Urban, Hong Kong	Nov, 2000 to Feb, 2001 and Jun, 2001 to Aug, 2001	5.71	10.12	0.89	1.92	Ho et al., 2006
Suburban, Hong Kong	Mar, 2011 to Feb, 2012	0.86	4.7	0.53	2.87	Huang et al., 2014b
Veneto, Italy	Apr 2012 to Feb 2013	1.3	5.5			Khan et al., 2016
Delhi, India	Dec 20, 2012 to Feb 26, 2013	12.04	16.46	4.43	6.61	Panda et al., 2016
Middle East (11 sampling sites in Palestine, Jordan and Israel)	Jan to Dec, 2007	2.1	5.3	2.2	4	Von Schneidmesser, et al., 2010 Abdeen, et al., 2014
Riyadh, Saudi Arabia	Apr to Sep, 2012	2.13	4.76	2.52	4.4	this study

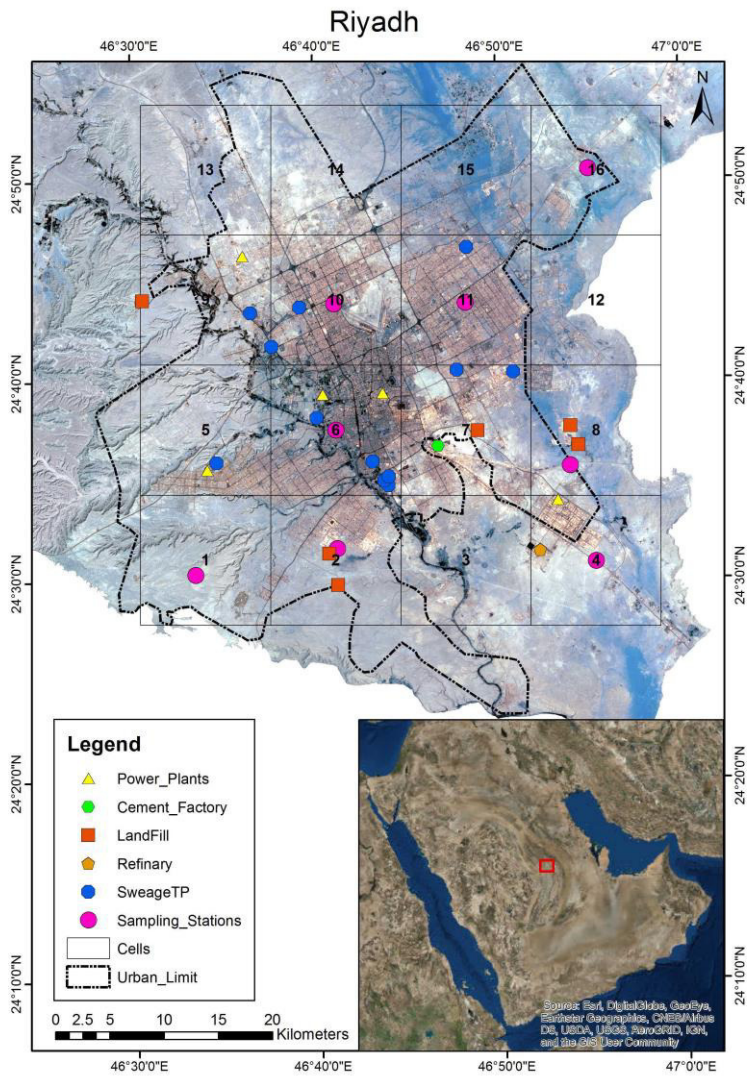
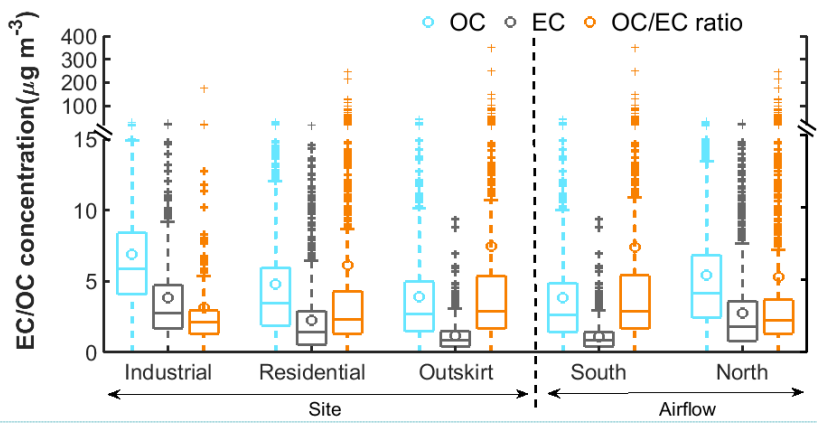
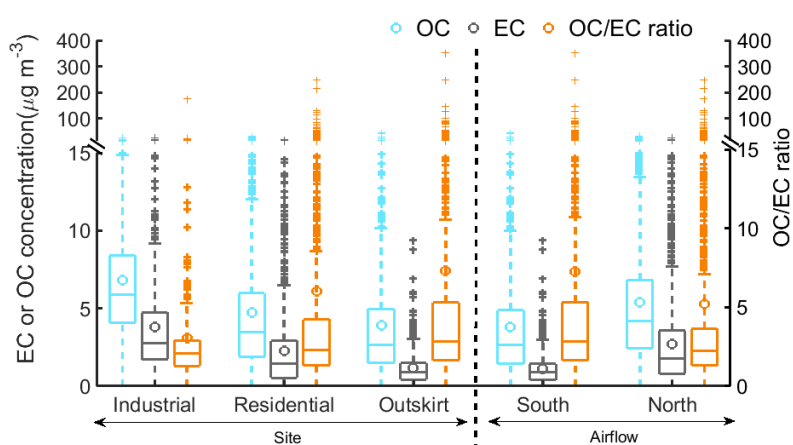


Figure 1 Image of Riyadh and immediate surroundings. Potential emission sources and 16 sampling locations are indicated. The characteristics of the sampling locations are listed in Table 1.

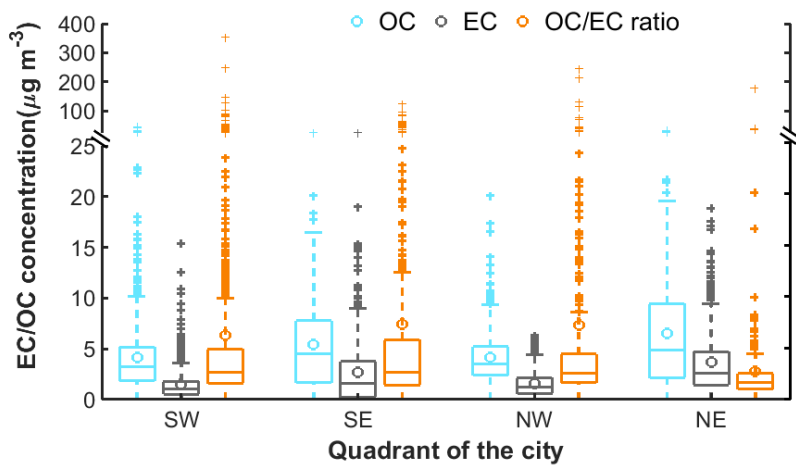


Formatted: Font: (Default) Arial, 12 pt

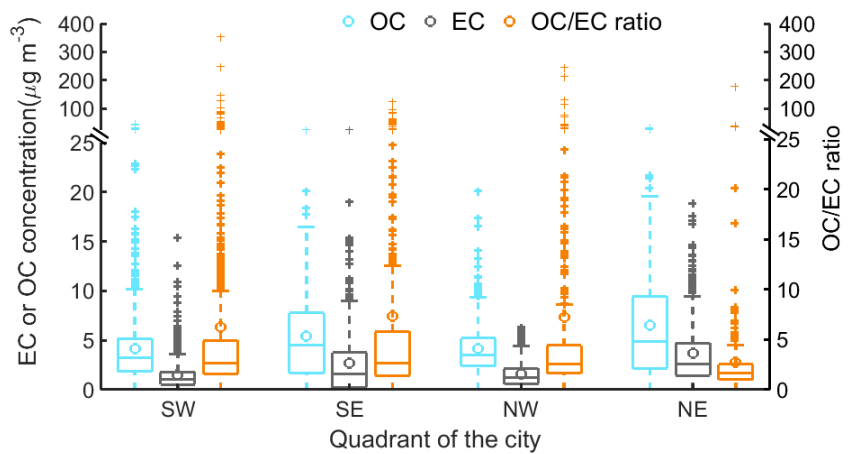


Formatted: Font: (Default) Arial, 12 pt

Figure 2 Observed OC and EC concentrations ($\mu\text{g m}^{-3}$) separated by site types and air mass source region according Table 1 and Figure 1b. Box and whisker plots show median and quartile values; averages are shown as circles and outliers as crosses.



Formatted: Font: (Default) Arial, 12 pt



Formatted: Font: (Default) Arial, 12 pt

Figure 3 Spatial variation of OC and EC concentrations ($\mu\text{g m}^{-3}$) and OC/EC ratios in each quadrant of Riyadh. SW represents southwest Riyadh and includes the sampling cells 1, 2, 5 and 6; SE represents southeast Riyadh and includes the cells 3, 4, 7, and 8; NW represents northwest Riyadh and includes the cells 9, 10, 13, and 14; and NE represents northeast Riyadh, and includes cells 11, 12, 15, and 16.

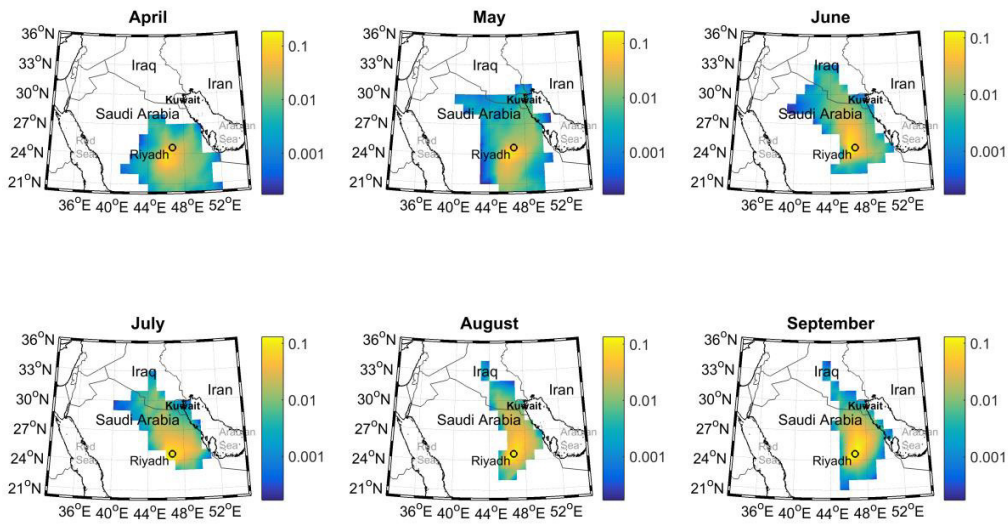
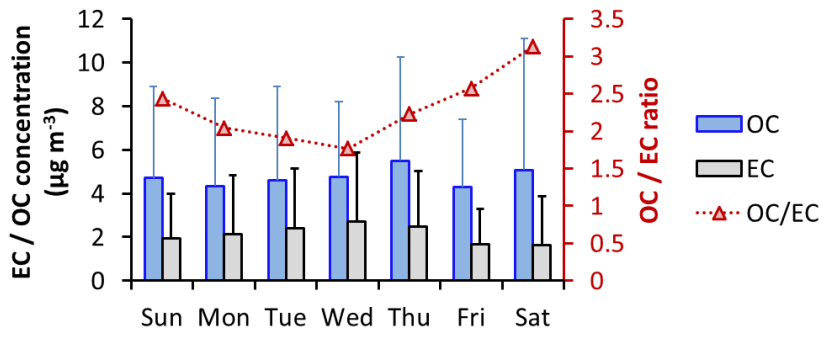
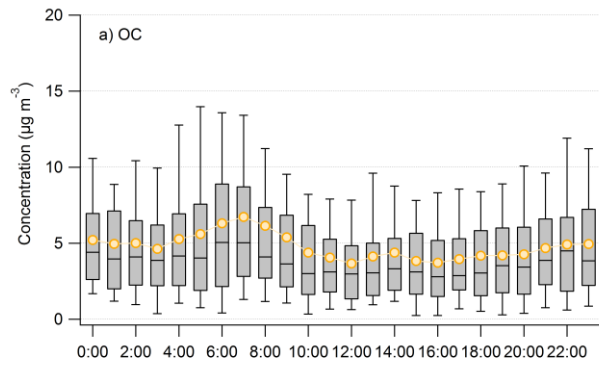


Figure 4 Back trajectory (24 h) residence time analysis of air masses arriving at Riyadh from April to September, 2011. Back trajectories were initiated from a starting height of 500 m above ground level. The color bar represents the normalized number count of the end points.

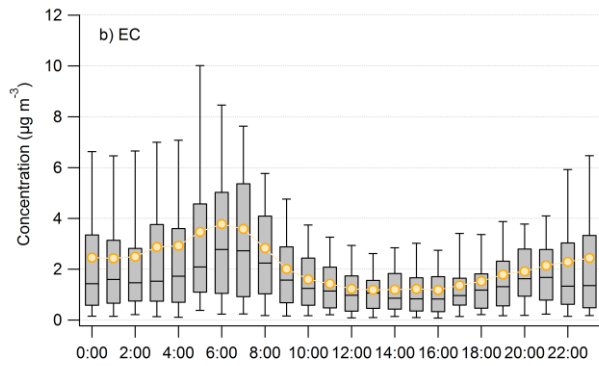


Formatted: Font: (Default) Arial, 12 pt

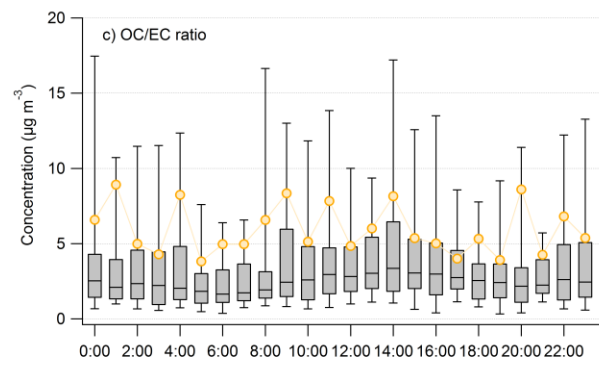
Figure 5 Day of week variation in OC ($\mu\text{g m}^{-3}$), EC ($\mu\text{g m}^{-3}$) and OC/EC ratio during the observational period.



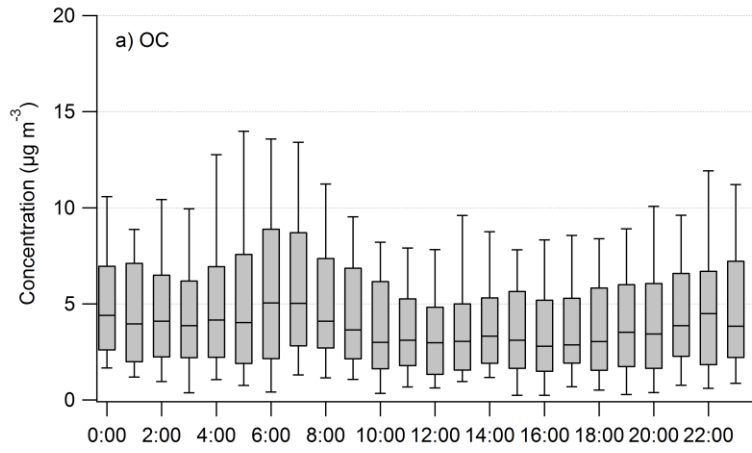
Formatted: Font: (Default) Arial, 12 pt



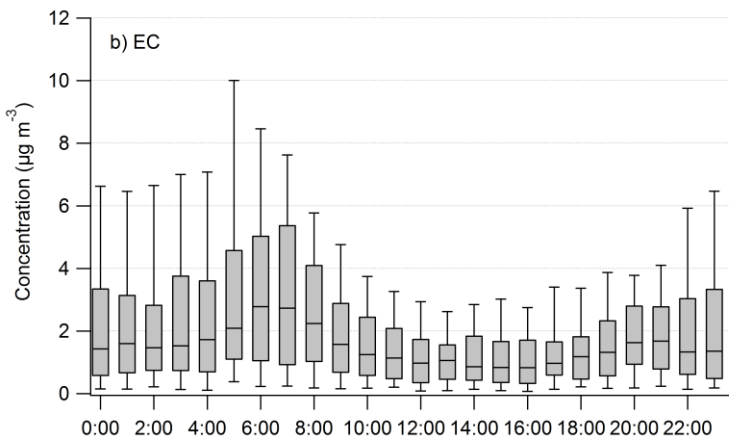
Formatted: Font: (Default) Arial, 12 pt



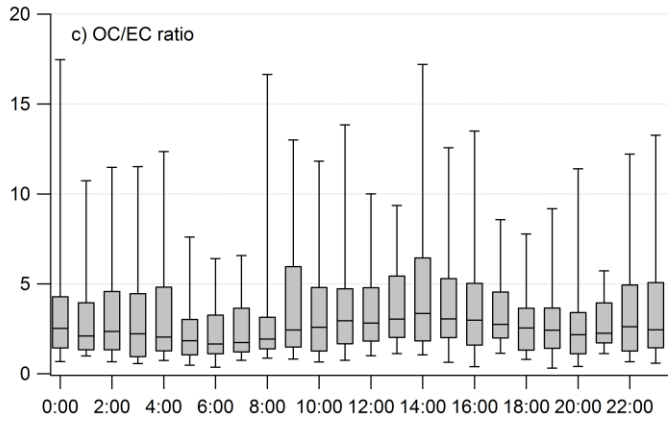
Formatted: Font: (Default) Arial, 12 pt



Formatted: Font: (Default) Arial, 12 pt

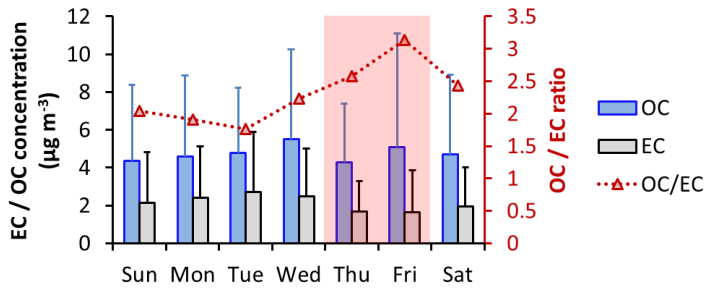


Formatted: Font: (Default) Arial, 12 pt



Formatted: Font: (Default) Arial, 12 pt

Figure 6-5 Diurnal variation of a) OC, b) EC and c) OC/EC ratio. Box and whisker plots show median represent the interquartile range and quartile the upper and lower whisker represent 90% and 10%, respectively values; averages are shown as orange circles.



Formatted: Font: (Default) Arial, 12 pt

Figure 6 Day-of-week variation in OC ($\mu\text{g m}^{-3}$), EC ($\mu\text{g m}^{-3}$) and OC/EC ratio during the observational period. The shading days (Thu and Fri) were the weekends in Saudi Arabia in 2012.

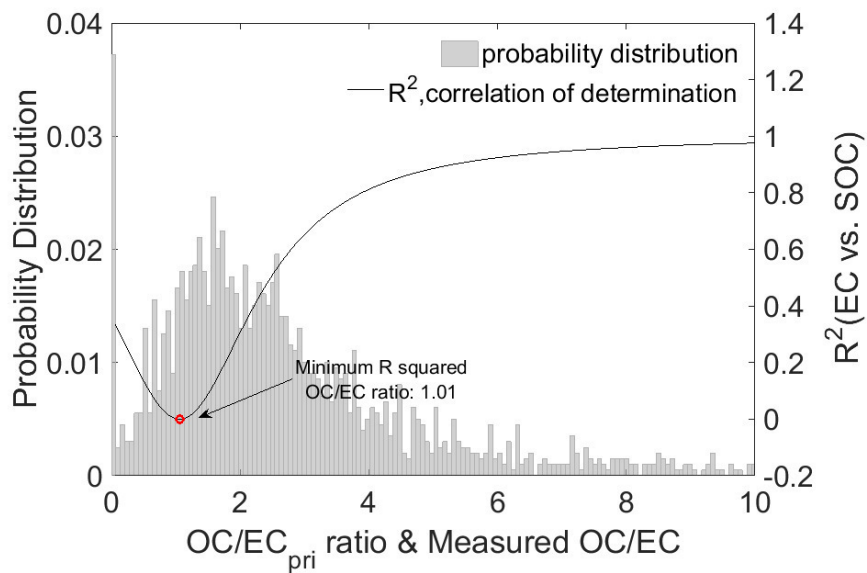


Figure 7 Determination of $(OC/EC)_{pri}$ using the minimum R squared method (MRS). The black curve is the coefficient of determination (R^2) between SOC and EC as a function of the assumed primary OC/EC ratio. The grey shaded area represents the probability distribution of the measured OC / EC ratios. The turning point (red circle) in the curve gives the best-fit primary emission ratio $(OC/EC)_{pri}$.

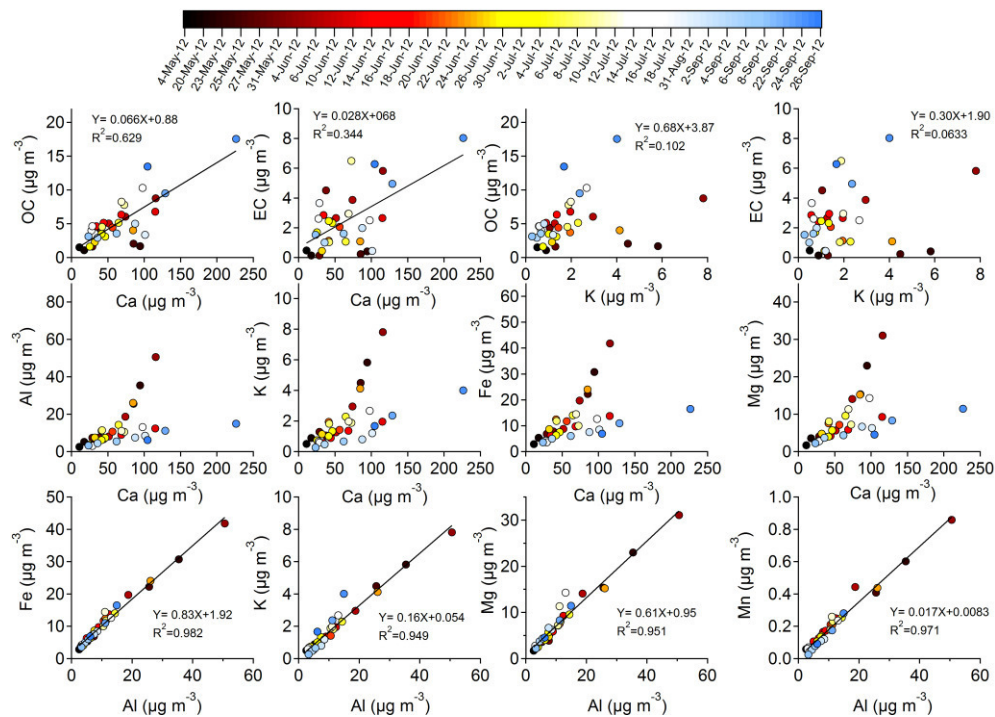


Figure 8 Correlation between dust species (Al, Fe, K, Mg, Mn and Ca), organic carbon (OC) and elemental carbon (EC) concentrations (μg m⁻³). Color bar represents the corresponding sampling date.

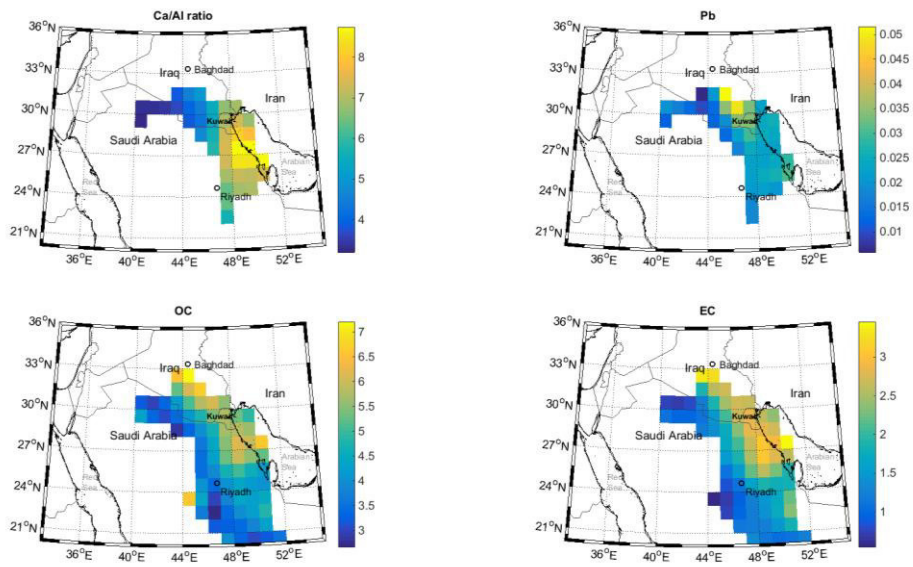


Figure 9 Concentration weighted trajectory analysis for indicated species, for 24-hr back trajectories with a starting height of 500 m. Color bars represent Ca/Al ratio, Pb concentrations (ng m^{-3}), OC concentrations ($\mu\text{g m}^{-3}$), and EC concentrations ($\mu\text{g m}^{-3}$).

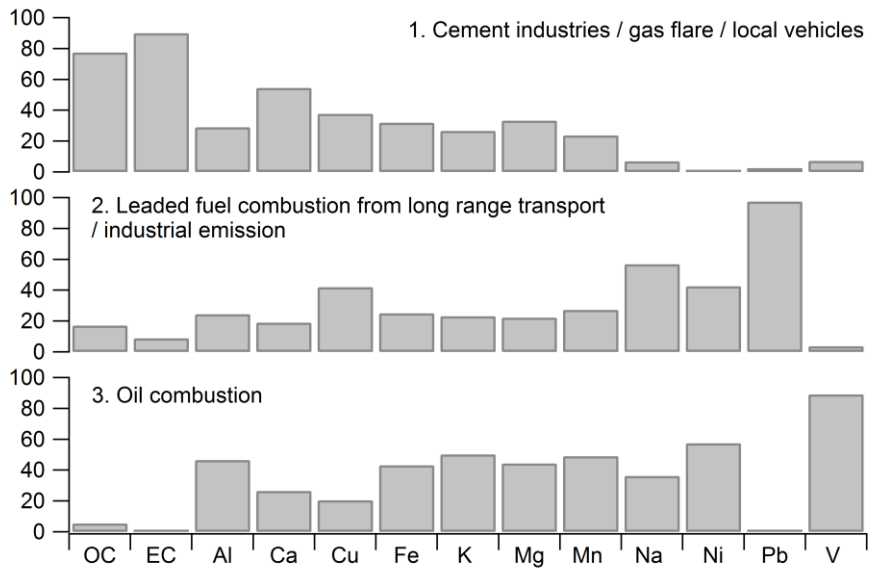
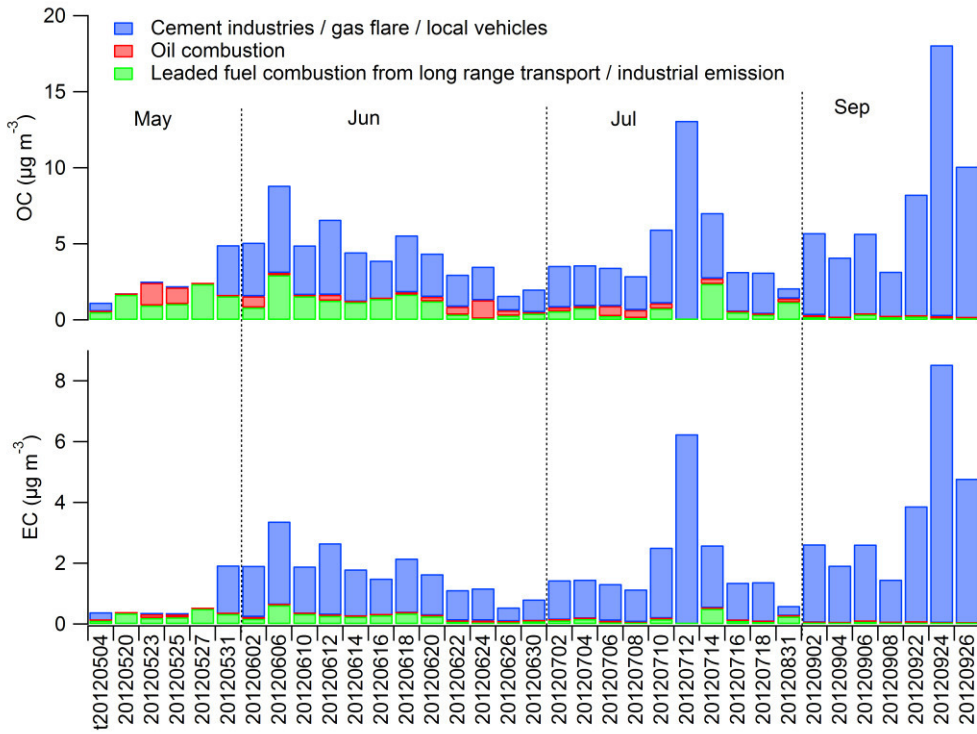
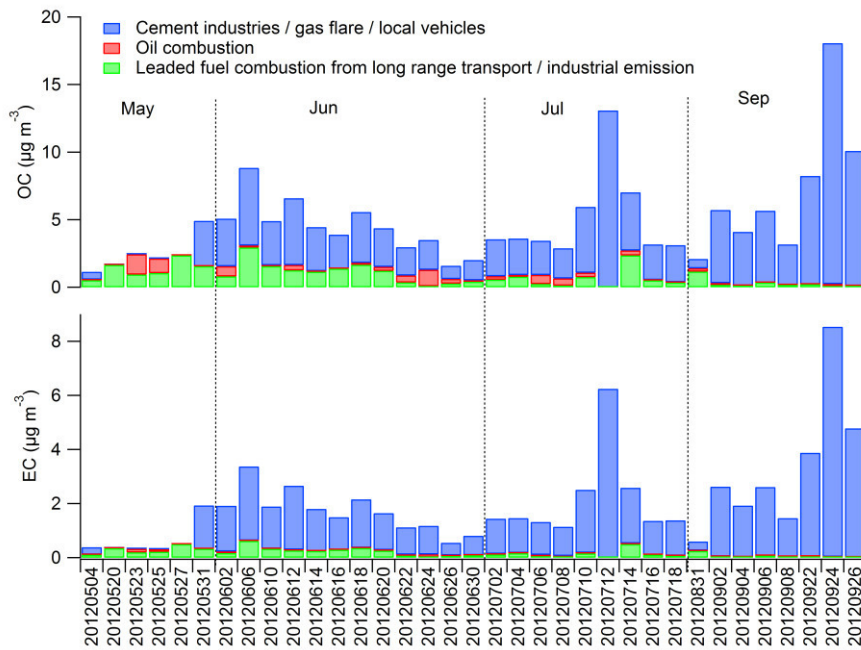


Figure 10 Source profile of PMF analysis of combined $PM_{2.5}$ OC and EC and PM_{10} metals concentrations. The sum of the species for all the factors was normalized to unity.



Formatted: Font: (Default) Arial, 12 pt



Formatted: Font: (Default) Arial, 12 pt

Figure 11 Source contributions to (a) OC and (b) EC ($\mu\text{g m}^{-3}$) from three sources, for each sample.

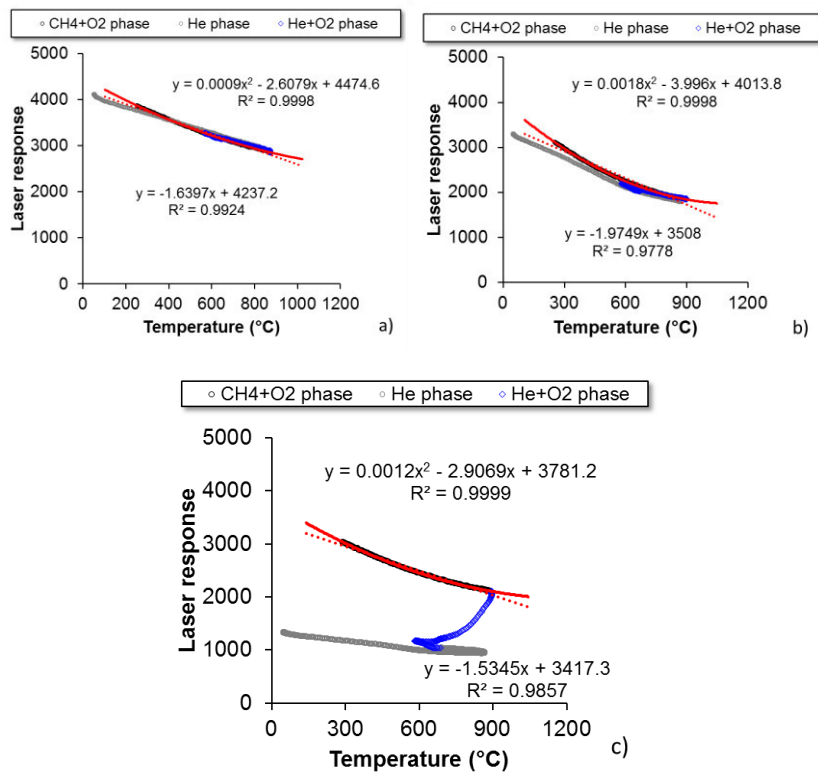


Figure A.1: Correlation between laser response and temperature (°C) for the three samples whose thermograms are shown in Figure A.2. (a) blank at 00:15 am, 20120706; (b) ambient sample at 20:00 pm, 20120706 (c) ambient sample at 6:00 am, 20120709. The gray lines indicate points during the oxygen-free (He only) phase of the analysis, the blue line is for points during the oxidizing stage (He+O₂) of the analysis and the black line is for the points during the calibration stage (CH₄+O₂). The red line is a best-fit polynomial through the CH₄+O₂ points, while the dashed red lines are linear fits.

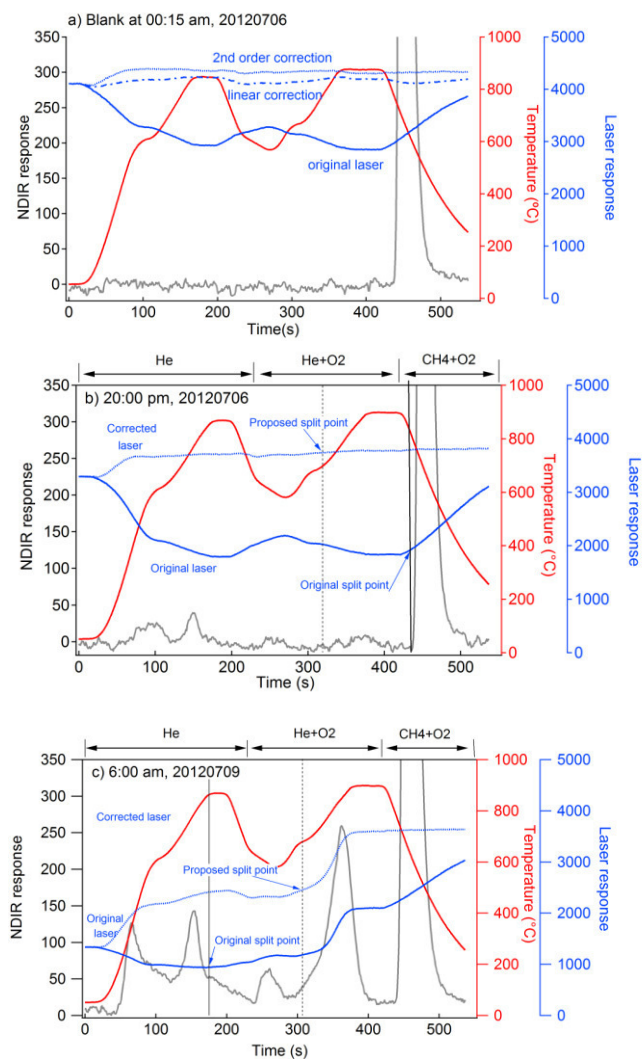


Figure A.2: Thermograms of selected Riyadh samples: (a) blank at 00:15 am, 20120706 (YYYYMMDD); (b) ambient sample at 20:00 pm, 20120706 with relatively low EC loading; (c) ambient sample at 6:00 am, 20120709 with relatively high EC loading.

Sources of PM_{2.5} carbonaceous aerosol in Riyadh, Saudi Arabia

*Qijing Bian¹, Badr Alharbi², Mohammed M. Shareef², Tahir Husain², Mohammad J. Pasha¹,
Sam. A. Atwood¹, Sonia M. Kreidenweis^{1,*}*

¹Department of Atmospheric Science, Colorado State University, Fort Collins, CO, 80526, USA.

²National Center for Environmental Technology, King Abdulaziz City for Science and
Technology, P.O. Box 6086, Riyadh 11442, Saudi Arabia.

³Faculty of Engineering and Applied Science, Memorial University, St. John's, NL, A1B 3X5
Canada.

*Corresponding author: bianqj@atmos.colostate.edu and sonia@atmos.colostate.edu

Table S1 Summary of sampling sites, dates and average concentration ($\mu\text{g m}^{-3}$) for OC and EC measurements (after Alharbi et al. 2014). Grid cells are shown in Figure 1.

Sampling cell	Designation	Type	Approx. number industrial sources	Cycle 1	Cycle 2	OC ¹	EC ¹
1	SW corner, semirural	Outskirts	9	Apr 8-14, 16-24, 28-30; May 1-5, 7-15, 20-21		3.84±4.27	1.14±1.06
2	Residential and some small scale industrial area (suburban area)	Residential	187		Jul 3-8	4.83±1.95	1.73±1.37
3	Moderately populated residential area with car salvage yards and some agricultural farms (suburban area)	Residential	25	May 22-27		1.56±1.54	0.24±0.26
4	Industrial area (urban area)	Industrial	658		Jul 9-14	8.53±3.63	4.45±3.47
5	Residential densely populated area (urban area)	Residential	102	May 30-31, June 2		6.07±7.90	3.36±2.17
6	Commercial, industrial and residential very densely populated area with city sewage wastewater treatment plants (urban area)	Residential	344		Jul 15-19	4.35±3.27	2.89±2.45
7	Industrial and residential area with a cement factory situated in this area with continual stone crushing operations activities (urban area)	Industrial	289	Jun 3, 5-8		7.27±1.86	5.07±3.43
8	Semi industrial area with commercial train route passing through (suburban area)	Industrial	20		Aug 28-31, Sep 1-2	5.58±4.67	2.74±3.43
9	Residential area mostly covered with agricultural land (suburban area)	Residential	12	Jun 9-14		6.52±3.63	2.64±1.67
10	Residential area (urban area)	Residential	130		Sep 3-8	3.34±1.30	1.51±0.96
11	Residential and semi industrial area with number of automobile workshops (urban area)	Industrial	394	Jun 15-20		5.18±2.88	3.03±2.28

12	This area is considered a residential area with a number of automobile workshops (suburban area)	Residential	0		Sep 10-14	N/A	N/A
13	Semi background/residential area (semirural area)	Residential	5	Jun 21-26		3.22±2.19	0.93±0.88
14	Residential area with extended construction activities (suburban area)	Residential	8		Sep 15-20	N/A	N/A
15	Residential area (suburban area)	Residential	44	June 28-Jul 2		1.78±1.51	1.71±1.40
16	Semi background with small populated residential area and large non-agricultural vacant land (semirural area)	Residential	4		Sep 21-26	12.49±5.30	6.44±4.00

¹ OC/EC filters were changed after the laser intensity was reduced to 2000 or 3000 [a.u.]

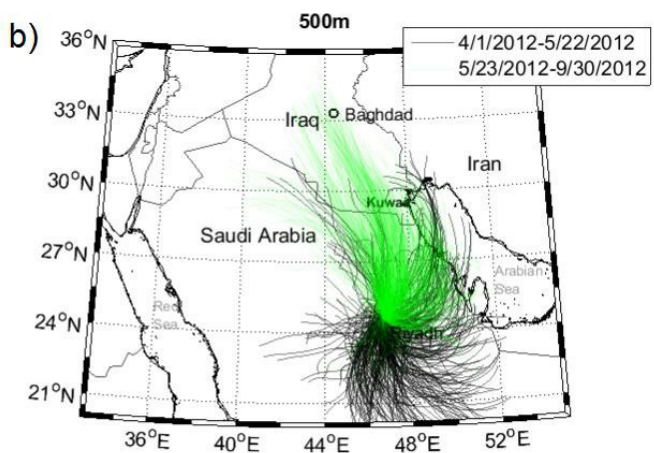
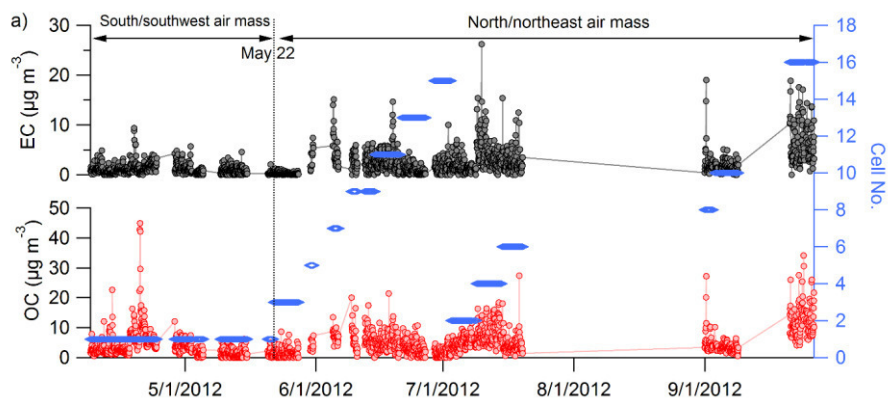
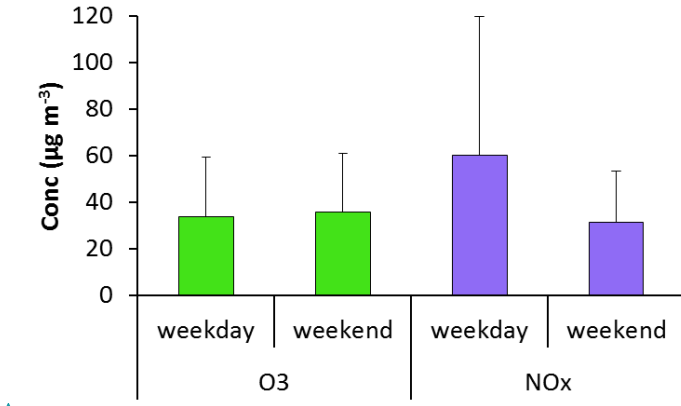
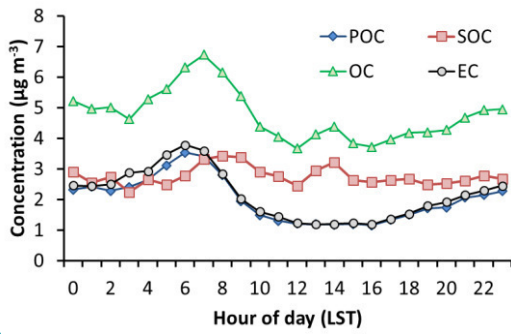


Figure S1: a) Time series of OC and EC measurements and the corresponding sampling cells at Riyadh in 2012; b) 24 hr back trajectories (starting height of 500 m) for the sampling period April 1 – May 22 (black lines) and May 23 – September 30 (green lines), 2012.

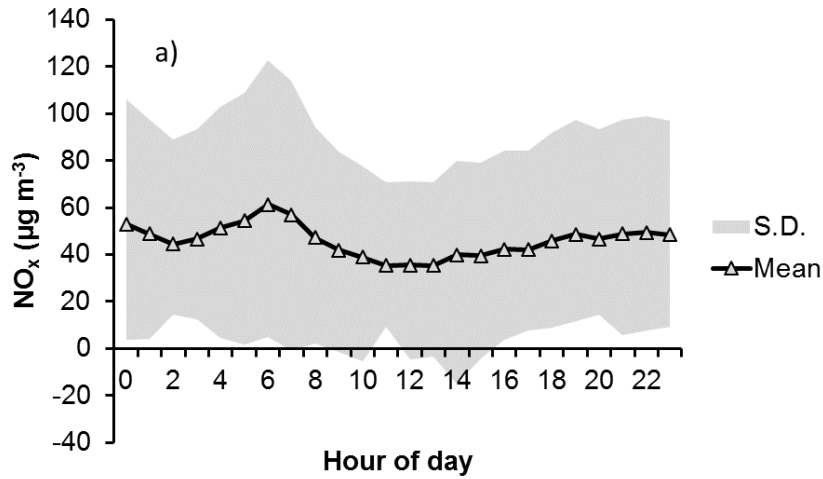


Formatted: Font: Arial, 12 pt

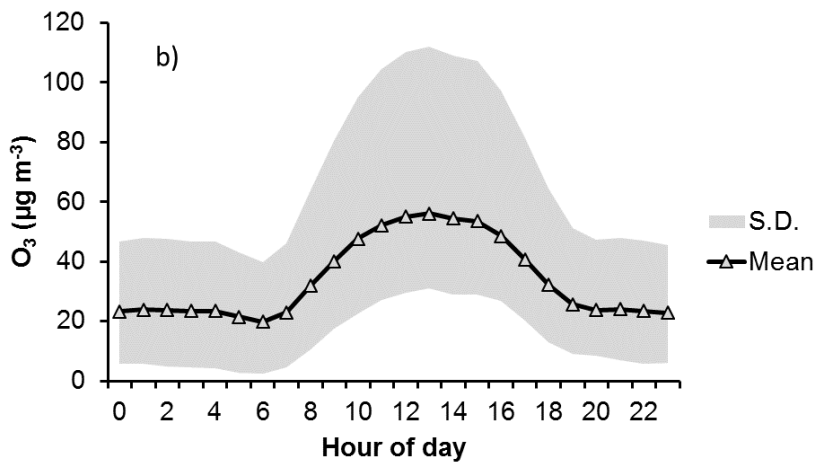
Figure S2 Weekday-weekend variation of O₃ and NO_x concentrations (µg m⁻³).



Formatted: Font: Arial, 12 pt



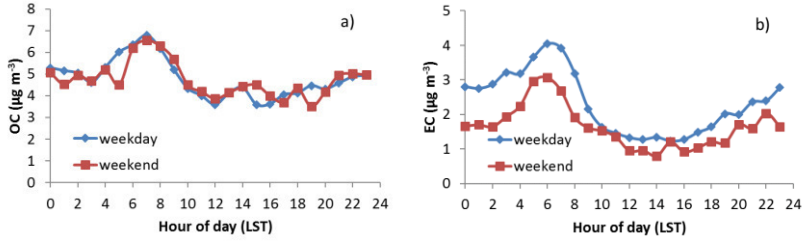
Formatted: Font: Arial, 12 pt



Formatted: Font: Arial, 12 pt

Figure S42: Hourly variation of a) NO_x and b) O₃ (µg m⁻³) during the observational periods.

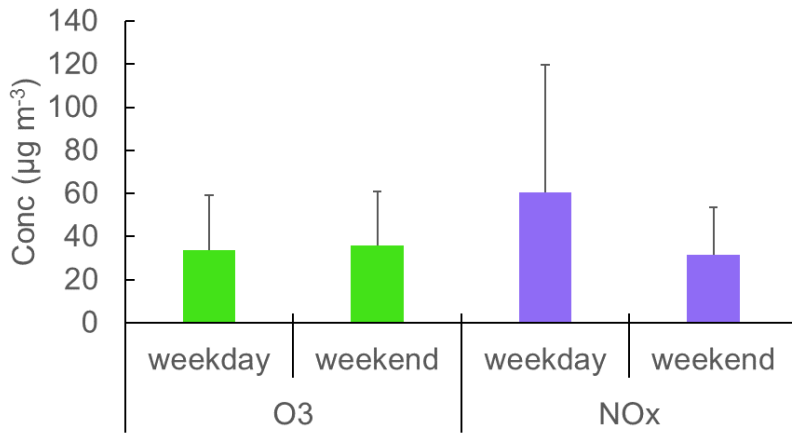
Figure S3 Diurnal variation of POC, SOC, OC and EC concentrations ($\mu\text{g m}^{-3}$), averaged over all



Formatted: Font: Arial, 12 pt

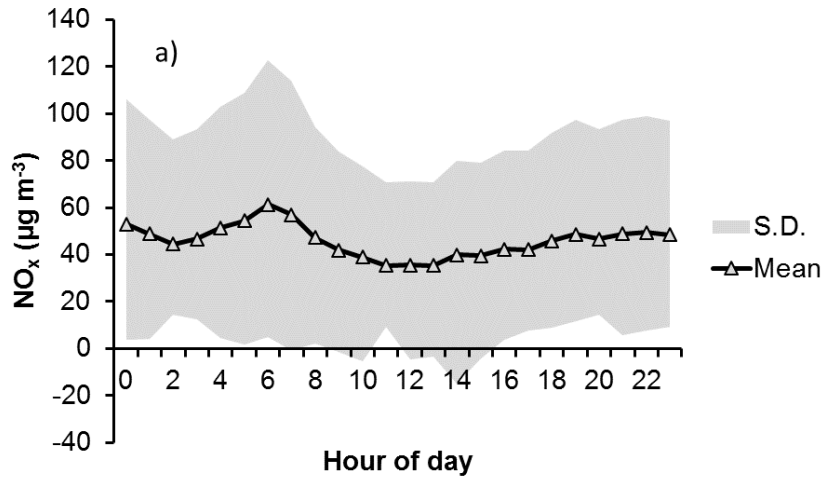
Formatted: Font: Arial, 12 pt

Figure S3: Diurnal variation of POC, SOC, OC and EC concentrations ($\mu\text{g m}^{-3}$) on the weekdays and weekends.

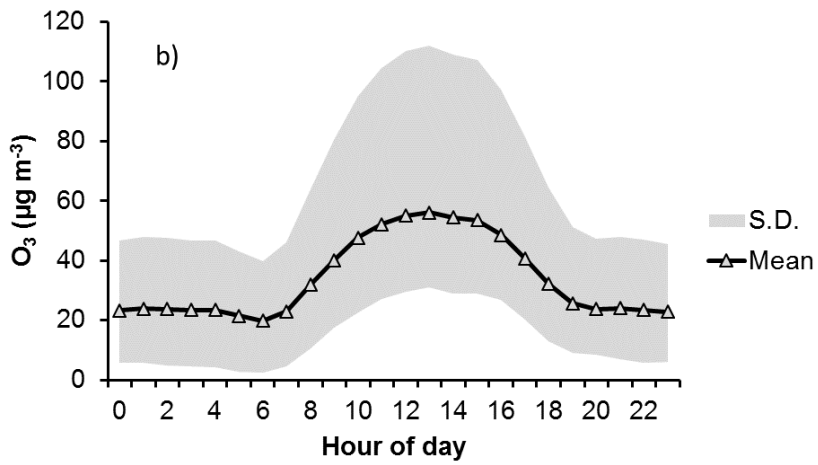


Formatted: Font: Arial, 12 pt

Figure S4: Weekday-weekend variation of O_3 and NO_x concentrations ($\mu\text{g m}^{-3}$).

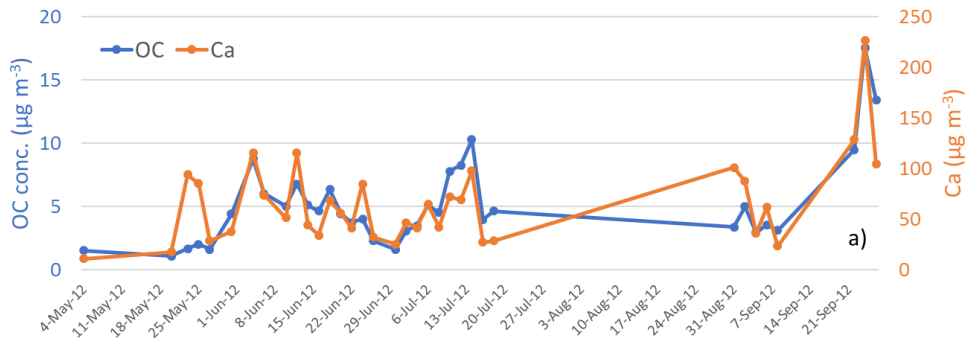


Formatted: Font: Arial, 12 pt

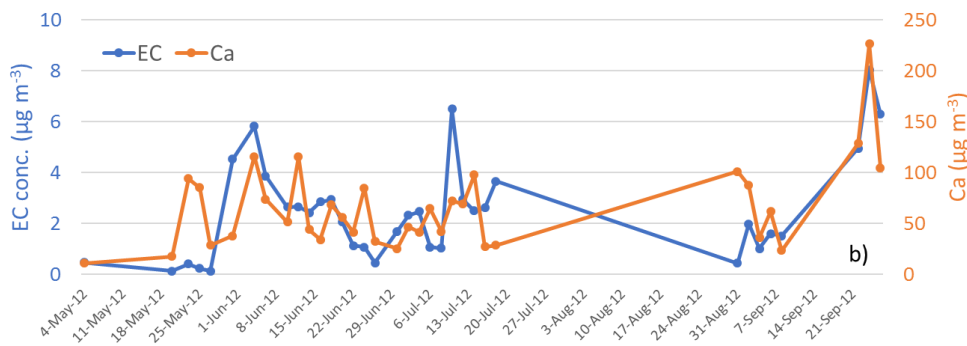


Formatted: Font: Arial, 12 pt

Figure S4 Hourly variation of a) NO_x and b) O_3 ($\mu\text{g m}^{-3}$) during the observational periods.



Formatted: Font: Arial, 12 pt



Formatted: Font: Arial, 12 pt

Figure S5: a) Time series of daily-average OC and Ca ($\mu\text{g m}^{-3}$) and b) time series of daily-average EC and Ca ($\mu\text{g m}^{-3}$)

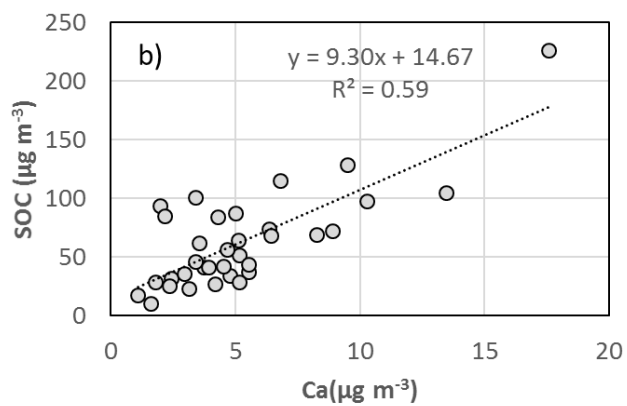
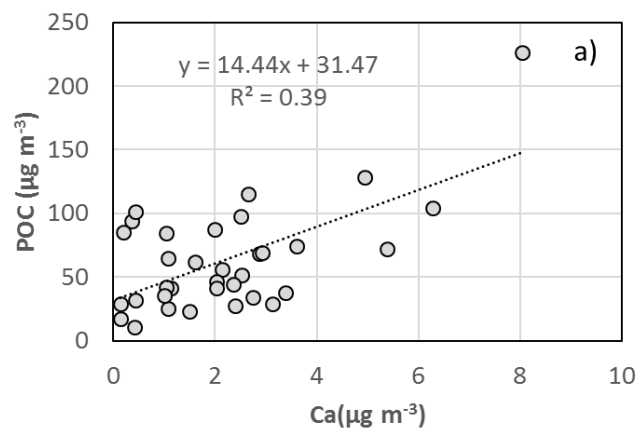


Figure S5-S6: a) Correlation between POC and Ca ($\mu\text{g m}^{-3}$) and b) correlation between SOC and Ca ($\mu\text{g m}^{-3}$)

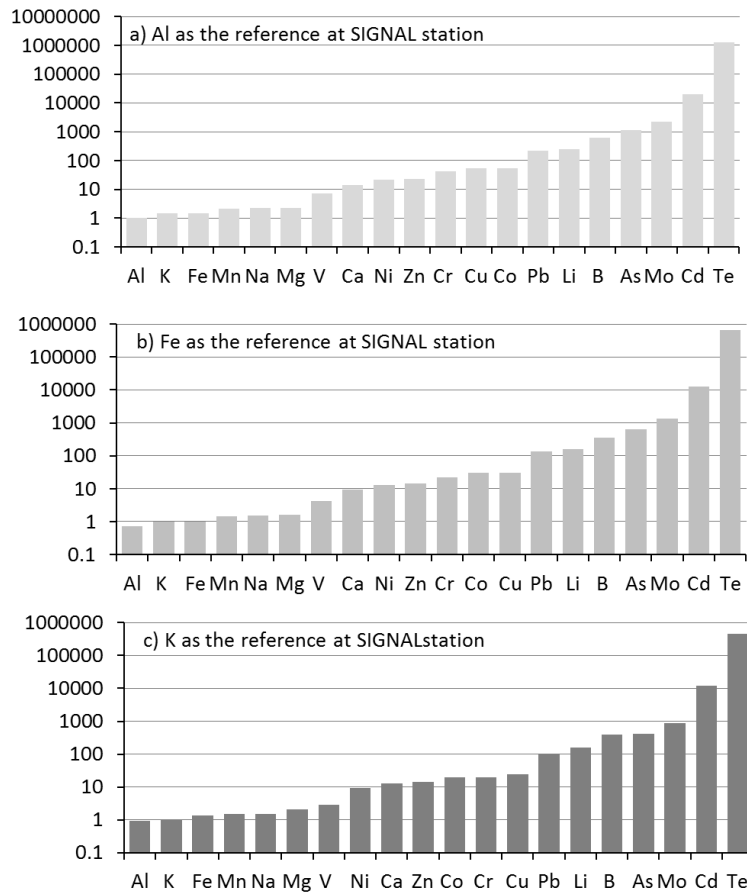


Figure S6-S7: Enrichment factor calculation a) using Al as the reference species; b) using Fe as the reference species; c) using K as the reference species.

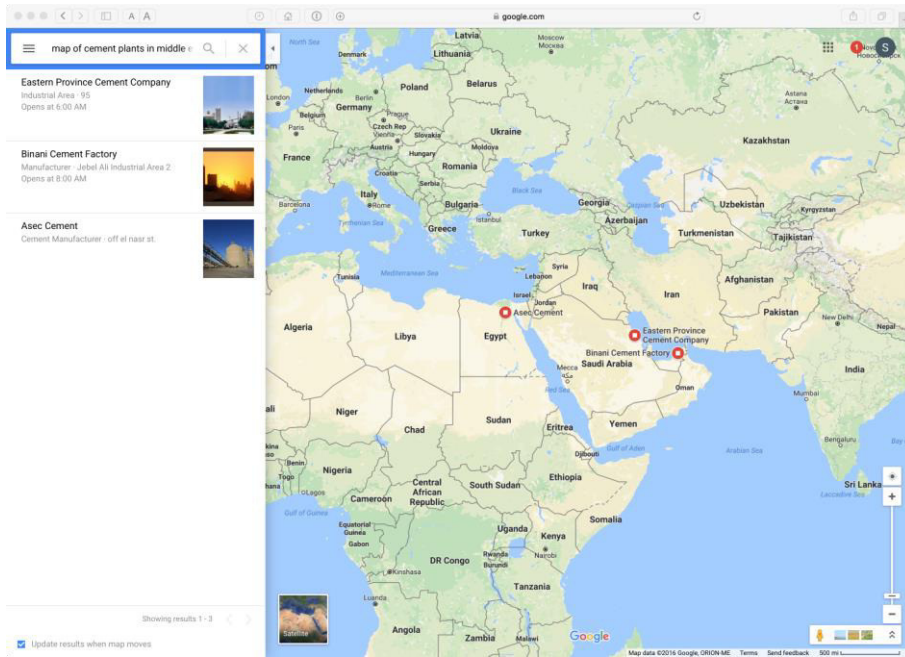


Figure S7-S8: Locations of cement plants, via a search in Google Maps.



Figure S8S9: Map indicating the distribution of oil or gas fields and refineries. Available at: <http://www.silverbearcafe.com/private/11.10/images/nigelmaund102010A.jpg>